

The oxidative stress response and virulence of pathogenic Leptospira are controlled by the interplay of two peroxide stress regulators

Crispin Zavala-Alvarado, Antony T. Vincent, Odile Sismeiro, Rachel Legendre, Hugo Varet, Giovanni Bussotti, Céline Lorioux, Jean-Yves Coppée, Frédéric J. Veyrier, Mathieu Picardeau, et al.

▶ **To cite this version:**

Crispin Zavala-Alvarado, Antony T. Vincent, Odile Sismeiro, Rachel Legendre, Hugo Varet, et al.. The oxidative stress response and virulence of pathogenic Leptospira are controlled by the interplay of two peroxide stress regulators. 2021. pasteur-03250968

HAL Id: pasteur-03250968
https://pasteur.hal.science/pasteur-03250968

Preprint submitted on 5 Jun 2021

HAL is a multi-disciplinary open access archive for the deposit and dissemination of scientific research documents, whether they are published or not. The documents may come from teaching and research institutions in France or abroad, or from public or private research centers.

L'archive ouverte pluridisciplinaire **HAL**, est destinée au dépôt et à la diffusion de documents scientifiques de niveau recherche, publiés ou non, émanant des établissements d'enseignement et de recherche français ou étrangers, des laboratoires publics ou privés.



Distributed under a Creative Commons Attribution 4.0 International License

bioRxiv preprint doi: https://doi.org/10.1101/2020.11.06.371039; this version posted November 6, 2020. The copyright holder for this preprint (which was not certified by peer review) is the author/funder, who has granted bioRxiv a license to display the preprint in perpetuity. It is made available under aCC-BY 4.0 International license.

The oxidative stress response and virulence of pathogenic *Leptospira* are controlled by the interplay of two peroxide stress regulators

Short title: Identification of a second PerR-like regulator in pathogenic *Leptospira*.

Crispin Zavala-Alvarado[1§#], Antony T. Vincent[2], Odile Sismeiro[3], Rachel Legendre[3,4], Hugo Varet[3,4], Giovanni Bussotti[4], Céline Lorioux[1], Jean-Yves Coppée[3], Frédéric J. Veyrier[2], Mathieu Picardeau[1], and Nadia Benaroudj[1]*

[1] Unité de Biologie des Spirochètes, Department of Microbiology, Institut Pasteur, Paris, France

[2] INRS-Centre Armand-Frappier, Bacterial Symbionts Evolution, Laval, Québec, Canada

[3] Biomics technological plateform, Center for Technological Resources and Research, Institut Pasteur, Paris, France

[4] Bioinformatics and Biostatistics Hub, Department of Computational Biology, USR 3756 CNRS, Institut Pasteur, Paris, France

[§] Université de Paris, Sorbonne Paris Cité, COMUE BioSPC, Paris 75013, France

[#] Current address: Microbial Individuality and Infection group, Department of Cell Biology and Infection, Institut Pasteur, Paris, France

* Corresponding author, E-mail: nadia.benaroudj@pasteur.fr (NB)

bioRxiv preprint doi: https://doi.org/10.1101/2020.11.06.371039; this version posted November 6, 2020. The copyright holder for this preprint (which was not certified by peer review) is the author/funder, who has granted bioRxiv a license to display the preprint in perpetuity. It is made available under aCC-BY 4.0 International license.

Keywords: Microbiology; transcription regulation; reactive oxygen species (ROS); oxidative stress; virulence; leptospirosis; RNASeq; non-coding RNAs; *Leptospira*; Spirochetes; PerR; Fur

Abstract

Pathogenic *Leptospira* are the causative agents of leptospirosis, the most widespread zoonotic infectious disease. Leptospirosis is a potentially severe and life-threatening emerging disease with highest burden in sub-tropical areas and impoverish populations. Mechanisms allowing pathogenic *Leptospira* to survive inside a host and induce acute leptospirosis are not fully understood. The ability to resist deadly oxidants produced by the host during infection is pivotal for *Leptospira* virulence. We have previously shown that genes encoding defenses against oxidants in *L. interrogans* are repressed by PerRA (encoded by LIMLP_10155), a peroxide stress regulator of the Fur family. In this study, we describe the identification and characterization of another putative PerR-like regulator (LIMLP_05620) in *L. interrogans*. Protein sequence and phylogenetic analyses indicated that LIMLP_05620 displayed all the canonical PerR amino acid residues and is restricted to pathogenic *Leptospira* clades. We therefore named this PerR-like regulator PerRB. In *L. interrogans*, the PerRB regulon is distinct from that of PerRA. While a *perRA* mutant had a greater tolerance to peroxide, inactivating *perRB* led to a higher tolerance to superoxide, suggesting that these two regulators have a distinct function in the adaptation of *L. interrogans* to oxidative stress. The concomitant inactivation of *perRA* and *perRB* resulted in a higher tolerance to both peroxide and superoxide and, unlike the single mutants, to the loss of *Leptospira* virulence. Interestingly, this correlated with major changes in gene and non-coding RNA expression, only observed in the double *perRAperRB* mutant. Notably, several virulence-associated genes (*clpB*, *ligA/B*, and *lvrAB*) were repressed. By obtaining the first double mutant in a pathogenic

bioRxiv preprint doi: https://doi.org/10.1101/2020.11.06.371039; this version posted November 6, 2020. The copyright holder for this preprint (which was not certified by peer review) is the author/funder, who has granted bioRxiv a license to display the preprint in perpetuity. It is made available under aCC-BY 4.0 International license.

Leptospira strain, our study has uncovered for the first time the interplay of two PerRs, not only in the adaptation of *Leptospira* to oxidative stress, but also in their virulence and pathogenicity, most likely through the transcriptional control of a complex regulatory network.

Author summary

Leptospirosis is a widespread infectious disease responsible for over one million of severe cases and 60 000 fatalities annually worldwide. This neglected and emerging disease has a worldwide distribution, but it mostly affects populations from developing countries in sub-tropical areas. The causative agents of leptospirosis are pathogenic bacterial *Leptospira* spp. There is a considerable deficit in our knowledge of these atypical bacteria, including their virulence mechanisms. In addition to the *Leptospira* PerRA regulator that represses defenses against peroxide, we have identified and characterized a second PerR regulator in pathogenic *Leptospira* species (PerRB) that participates in *Leptospira* tolerance to superoxide. Phenotypic and transcriptomic analyses of single PerRA and PerRB mutants suggest that the two PerRs fulfill distinct functions in the adaptation to oxidative stress. However, concomitant inactivation of PerRA and PerRB resulted in a higher tolerance to both peroxide and superoxide, but to a loss virulence.

The absence of the two PerR regulators resulted in global and major changes in the transcriptional profile, including a dramatic decrease of several virulence factor expression. Our study has demonstrated that PerRA and PerRB cooperate to orchestrate a complex regulatory network involved in *Leptospira* virulence.

bioRxiv preprint doi: https://doi.org/10.1101/2020.11.06.371039; this version posted November 6, 2020. The copyright holder for this preprint (which was not certified by peer review) is the author/funder, who has granted bioRxiv a license to display the preprint in perpetuity. It is made available under aCC-BY 4.0 International license.

Introduction

Pathogenic *Leptospira* spp. are aerobic Gram-negative bacteria of the spirochetal phylum that are the causative agents of leptospirosis, the most widespread zoonosis [1]. More than one million cases of leptospirosis are currently reported annually in the world, with 10% of mortality [2]. This disease is considered as a health threat among impoverished populations in developing countries under tropical areas [2], but the number of reported cases of leptospirosis are also on the rise in developed countries under temperate climates [3]. Rodents are asymptomatic reservoir for leptospires as the bacteria colonize the proximal renal tubules of these animals. Leptospires are shed in the environment through the urine of infected animals and leptospirosis is transmitted to other animal species and humans mostly by exposure to contaminated soils and water. *Leptospira* penetrate an organism through abraded skins and mucous membranes, subsequently disseminate within the bloodstream and rapidly spread to multiple tissues and organs (including kidney, liver, lungs). Clinical manifestations range from a mild flu-like febrile state to more severe and fatal cases leading to hemorrhages and multiple organ failure. Because of the lack of efficient tools for genetic manipulation of *Leptospira* spp. and their fastidious growth in the laboratory conditions, our understanding of the mechanism of pathogenicity and virulence as well as the basic biology of these pathogens have been greatly hampered [4,5].

During their life cycle, most bacteria will be exposed to reactive oxidative species (ROS), such as superoxide anion ($^{\bullet}O_2^-$) and hydrogen peroxide (H_2O_2), that are produced endogenously or encountered in the environment [6]. The superoxide is formed during the aerobic respiratory chain upon the reduction of the dioxide (O_2). Dismutation of superoxide will give rise to H_2O_2 which, in turn, can react with ferrous iron to generate the highly reactive hydroxyl radicals ($^{\bullet}OH$) through the Fenton reaction. These ROS are also produced

bioRxiv preprint doi: https://doi.org/10.1101/2020.11.06.371039; this version posted November 6, 2020. The copyright holder for this preprint (which was not certified by peer review) is the author/funder, who has granted bioRxiv a license to display the preprint in perpetuity. It is made available under aCC-BY 4.0 International license.

together with hypochlorous acid (HOCl), and nitric oxide anion ($^{\bullet}$NO) as powerful and efficient weapons by eukaryotic innate immune response upon infection by pathogenic bacteria [7]. ROS cause oxidative damage to cellular components (proteins, DNA and lipids) and this would result in bacterial death if bacteria had not developed scavenging enzymes to counteract the deadly effect of ROS, including catalase, peroxidases and superoxide dismutase or reductase (SOD, SOR). Indeed, in response to any increase in ROS concentration, as occurred during environmental oxidative stress or when infecting a host, bacteria trigger an adaptive response allowing the fine-tuning of scavenging enzyme synthesis rate that appropriately adapts the defenses against ROS to the oxidant assault. ROS production is increased upon infection by *Leptospira* [8] and with the development of severe leptospirosis in patients and infected animals [9,10]. In fact, the ability to detoxify H_2O_2 is essential for *Leptospira* virulence as inactivation of the catalase-encoding gene led to virulence attenuation in *L. interrogans* [11].

The oxidative stress adaptive response in bacteria is controlled by specialized ROS sensing transcription factors. OxyR and PerR are the main peroxide-sensing regulators found in Gram-negative and Gram-positive bacteria, respectively [12]. OxyR and PerR are functional equivalents but they do control expression of peroxide scavenging enzymes by different mechanisms. OxyR is a transcriptional regulator from the LysR family. Tetrameric OxyR binds promoters and activates the expression of genes coding for catalase and peroxidases through the oxidation of its H_2O_2 sensing cysteine residue [13,14]. PerR belongs to the Fur (Ferric uptake regulator) transcriptional factor family. It is a metalloprotein that binds DNA in the presence of iron or manganese and represses the expression of catalase and peroxidases [15–17]. In the presence of peroxide, PerR is oxidized on the histidine residues participating in iron coordination, PerR dissociates from DNA and peroxide-scavenging enzyme repression is alleviated [18,19]. In Gram-negative bacteria, SOD expression is controlled by the SoxRS

bioRxiv preprint doi: https://doi.org/10.1101/2020.11.06.371039; this version posted November 6, 2020. The copyright holder for this preprint (which was not certified by peer review) is the author/funder, who has granted bioRxiv a license to display the preprint in perpetuity. It is made available under aCC-BY 4.0 International license.

system [20,21] by a redox-sensing mechanism and oxidation of a Fe-S cluster [22]. In Gram-positive bacteria, SOD expression regulation probably involves the alternative Sigma Factor SigB among other mechanisms [23]. Pathogenic *Leptospira* spp. are among the few examples of Gram-negative bacteria where the expression of peroxide-scavenging enzymes is regulated by a PerR (encoded by LIMLP_10155/LIC12034/LA1857) and not an OxyR [24]. Moreover, their genomes do not contain any ORF encoding a SOD and they do not exhibit canonical SOD activity [25,26].

We have very recently characterized the transcriptional response to hydrogen peroxide in the pathogen *L. interrogans* and shown that these bacteria respond to sublethal H_2O_2 concentration by increasing the expression of catalase and of two peroxidases (Alkylperoxiredoxin (AhpC) and Cytochrome C peroxidase (CCP)) [27]. When *Leptospira* were exposed to deadly H_2O_2 concentration, additional enzymes with a putative role as antioxidants and/or in repair of oxidized cysteines in proteins were up-regulated, including several thiol oxidoreductases (thioredoxin, glutaredoxin, DsbD, and Bcp-like proteins) [27]. Several genes of the LexA regulon (*recA*, *recN*, *dinP*) and other genes with putative role in DNA repair (*mutS*, *radC*) had a higher expression as well as genes encoding for canonical chaperones (*dnaK/dnaJ/grpE*, *groES/EL*, and *hsp15/20*) [27]. Only genes coding for the catalase and peroxidases were under the control of PerR and our study has revealed a complex regulatory network independent of PerR involving other transcriptional regulators, sigma factors, two component systems and non-coding RNAs [27]. During the course of this study, we noticed that an ORF encoding a Fur-like regulator (LIMLP_05620/LIC11158/LA2887) was up-regulated when *Leptospira* were exposed to a deadly concentration of H_2O_2. Here, we report the functional characterization of this pathogenic *Leptospira*-specific Fur-like regulator in the adaptation of *Leptospira* to oxidative stress. Phenotypic analyses of a mutant inactivated in LIMLP_05620 indicates a role of this Fur-like regulator in *Leptospira* tolerance

bioRxiv preprint doi: https://doi.org/10.1101/2020.11.06.371039; this version posted November 6, 2020. The copyright holder for this preprint (which was not certified by peer review) is the author/funder, who has granted bioRxiv a license to display the preprint in perpetuity. It is made available under aCC-BY 4.0 International license.

147 to superoxide. This, together with the presence of the canonical amino acid residues of the
148 PerR DNA binding helix and H_2O_2 sensitivity, strongly suggest that LIMLP_05620 encodes a
149 second PerR-like regulator in pathogenic *Leptospira* species. By obtaining a double mutant
150 where LIMLP_05620 and *perR* (LIMLP_10155) are concomitantly inactivated, we have also
151 investigated the interplay between these two PerR-like regulators in the adaptation to
152 oxidative stress and virulence of *L. interrogans*. We have demonstrated a cooperation of
153 LIMLP_05620 with PerR in controlling several *Leptospira* virulence-associated genes,
154 including *ligA*, *ligB*, *lvrAB*, and *clpB*, perhaps illustrating the importance of functional
155 redundancy in pathogenic *Leptospira* virulence and pathogenicity.

bioRxiv preprint doi: https://doi.org/10.1101/2020.11.06.371039; this version posted November 6, 2020. The copyright holder for this preprint (which was not certified by peer review) is the author/funder, who has granted bioRxiv a license to display the preprint in perpetuity. It is made available under aCC-BY 4.0 International license.

Results

Identification of an ORF that encodes a novel putative PerR regulator in pathogenic *Leptospira* species.

Regulators of the Fur family are homodimeric metalloproteins with a two-domain organization composed of an amino-terminal DNA binding domain and a carboxy-terminal dimerization domain (Fig 1A). The DNA binding domain contains a winged helix-turn-helix (HTH) DNA binding motif (H2-H4, in Fig1A) where DNA binding is mediated by the H4 helix. The dimerization domain consists of an α/β domain. The regulatory iron that controls DNA binding and dissociation is coordinated by histidine, aspartate, and glutamate residues located in a loop at the hinge of the amino and carboxy-terminal domains. Most of Fur-like regulators also coordinate a structural metal (zinc) through 2 cysteinate motifs (CxxC, where x designates any AA). This structural metal allows correct folding and dimeric assembly of the regulator.

Due to a great conservation in protein folding, metal coordination and similarity in the metal-induced conformational switch controlling DNA binding, it is difficult to distinguish members of the Fur family on the sole basis of their primary sequence. However, in *B. subtilis*, a single amino acid residue in the H4 helix of the amino-terminal DNA binding domain (N61 and R61 for *B. subtilis* PerR and Fur, respectively) allows PerR and Fur to discriminate between their respective DNA sequence targets (PerR and Fur boxes, respectively) [28] (Fig 1B). In addition, D104 residue in the carboxy-terminal domain is pivotal in the PerR sensitivity to H_2O_2. The corresponding residue in Fur is a glutamate and mutating this residue in aspartate leads to H_2O_2 sensitivity [29] (Fig 1B). Therefore, N61 and D104 both allow to differentiate a PerR from a Fur in *B. subtilis* and the presence of these

bioRxiv preprint doi: https://doi.org/10.1101/2020.11.06.371039; this version posted November 6, 2020. The copyright holder for this preprint (which was not certified by peer review) is the author/funder, who has granted bioRxiv a license to display the preprint in perpetuity. It is made available under aCC-BY 4.0 International license.

canonical amino acid residues in PerR sequences is well-conserved in other bacterial species [28,29].

L. interrogans genome encodes 4 ORFs that share homology with regulators of the Fur family. Among those *Leptospira* Fur-like regulators, LIMLP_10155 is the only *Leptospira* Fur-like regulator that is functionally and structurally characterized. It encodes a PerR that represses genes encoding defenses against peroxide, including catalase and other peroxidases [24,27,30]. Our previous structural characterization of the PerR from *L. interrogans* indicates that this member of the Fur family lacks a structural metal binding site despite a correct folding and functional dimeric assembly [30].

Sequence alignment of these ORFs with the Fur and PerR from *B. subtilis* shows a good conservation of the two-domain organization and residues involved in the regulatory metal coordination (Fig 1B). Interestingly, two of the 4 Fur-like ORFs of *L. interrogans*, LIMLP_10155 (LIC12034/LA1857 encoding a PerR) and LIMLP_05620 (LIC11158/LA2887), exhibit the canonical asparagine (N60 and N68, respectively) and aspartate (D103 and D112, respectively) residues of a typical PerR. The third ORF encoding a putative Fur-like regulator, LIMLP_04825 (LIC11006/LA3094), possesses the two Fur typical residues, R76 and E121, respectively. The fourth ORF encoding a putative Fur-like regulator, LIMLP_18590 (LIC20147/LB183) possesses the typical Fur arginine residue in its putative H4 DNA binding helix (R51) but a typical PerR aspartate residue in the carboxy-terminal domain (D94). Of note, LIMLP_18590 has a glutamate residue at the position 96. Fold prediction suggests that the three Fur regulators encoded by LIMLP_05620, LIMLP_04825 and LIMLP_18590 adopt the two-domain organization typical of the Fur family depicted in the crystal structure of LIMLP_10155 (Fig 1C).

The closest relative of the PerR-encoding LIMLP_10155 is LIMLP_05620 with about 26% of sequence identity, and LIMLP_04825 and LIMLP_18590 are closest relatives that share 20%

bioRxiv preprint doi: https://doi.org/10.1101/2020.11.06.371039; this version posted November 6, 2020. The copyright holder for this preprint (which was not certified by peer review) is the author/funder, who has granted bioRxiv a license to display the preprint in perpetuity. It is made available under aCC-BY 4.0 International license.

206 of sequence identity. LIMLP_05620 shares about 27% identity with the well-characterized *B.*
207 *subtilis* PerR. The putative H4 helix in LIMLP_05620 (Leu63-Ser75) is relatively well
208 conserved with that of *B. subtilis* (Val56-Ser69) (Fig1B-C) and LIMLP_05620 displays a
209 typical regulatory metal coordination site (His44-Asp93-His99-His101-Asp112). As the
210 LIMLP_10155-encoded PerR, LIMLP_05620 lacks the cysteinate motif involved in structural
211 metal coordination [30] (Fig 1B). On the contrary, both LIMLP_04825 and LIMLP_18590
212 have one or two cysteinate motifs for structural metal coordination (C_{113}xxC_{116} and C_{86}xxC_{89}-
213 C_{122}xxC_{125}, respectively). Therefore, LIMLP_05620 encodes a putative PerR-like regulator
214 closely related to the PerR-encoding LIMLP_10155 whereas LIMLP_04825 and
215 LIMLP_18590 could encode other type of Fur-like regulators (Fur, Zur, or Nur). We therefore
216 annotated the LIMLP_10155 and LIMLP_05620 ORFs as *perRA* and *perRB*, respectively.
217
218 **Phylogenetic analysis of PerRA and PerRB in *Leptospira* species.**
219 To get a better understanding of the evolutionary relationship of the four Fur-like
220 regulators in pathogenic *Leptospira*, we undertook phylogenetic analyses by searching for
221 homologous sequences of the LIMLP_10155, LIMLP_05620, LIMLP_18590 and
222 LIMLP_04825 proteins among the representative genomes present in GenBank. This revealed
223 a large phylogenetic distribution with several branches (Fig 2A). The sequences homologous
224 to the LIMLP_04825 and LIMLP_18590 proteins form two distinct groups (red and orange,
225 respectively) separated by a common ancestor. To get better definition of phylogenetic
226 relationships of PerR-like homologues, we performed analysis with only a subset of sequence
227 (Fig 2B). This phylogenetic analysis shows two separated groups composed of the sequences
228 of LIMLP_10155 (PerRA) and LIMLP_05620 (PerRB) (see S1Fig for a more complete and
229 detailed tree).

bioRxiv preprint doi: https://doi.org/10.1101/2020.11.06.371039; this version posted November 6, 2020. The copyright holder for this preprint (which was not certified by peer review) is the author/funder, who has granted bioRxiv a license to display the preprint in perpetuity. It is made available under aCC-BY 4.0 International license.

The sequences of LIMLP_10155 and LIMLP_05620 ORFs from the strain *L. interrogans* serovar Manilae were searched and compared in all available genomes from the *Leptospira* genus (S1 Table). As seen in Fig 3, LIMLP_10155 is present in the saprophytes S1 and S2 clades and in the P1 clade (highly virulent strains). This ORF is absent from most of the P2 clade (intermediate strains). However, there are two exceptions in the P2 clade species since homologues of LIMLP_10155, which might have been acquired by a recent horizontal gene transfer, are present in *L. dzoumognesis* and *L. wolffii*. Additionally, this ORF is also present in other bacteria from the order *Leptospirales* such as *Turneriella parva* and *Leptonema illini* (Fig 2B). This suggests that LIMLP_10155 (PerRA) was present in *Leptospirales* ancestor before *Leptospira* divergence and lost in the P2 clade. On the other side, LIMLP_05620 ORF is only present in P1 and P2 clades and absent in all species from S1 and S2 clades (Fig 3). LIMLP_05620 is also not found in other bacteria from the *Leptospirales* order (Fig 2B and S1 Fig). This restricted distribution suggests that the ancestor of pathogenic strains (P1 and P2 clades) has likely acquired LIMLP_05620 after their divergence with other *Leptospira*. Overall, both PerR-encoding LIMLP_10155 and LIMLP_05620 ORFs only coexist in P1 clade that comprises the highly virulent *Leptospira* species. Altogether, these findings indicate that pathogenic *Leptospira* strains encode a second putative PerR-like regulator that is absent in saprophytes.

Role of PerRB in *L. interrogans* tolerance to ROS.

As demonstrated previously [27], when *L. interrogans* are exposed to a subtlethal dose of H_2O_2 (10 µM for 30 min) *perRA* expression is increased by a 7-fold whereas that of *perRB* is unchanged (Fig 4). In the presence of a higher dose of H_2O_2 (1 mM for 1h), expression of both *perRA* and *perRB* was increased significantly by a 6-fold (Fig 4). This suggests that PerRB, like PerRA, responds to deadly H_2O_2 dose.

bioRxiv preprint doi: https://doi.org/10.1101/2020.11.06.371039; this version posted November 6, 2020. The copyright holder for this preprint (which was not certified by peer review) is the author/funder, who has granted bioRxiv a license to display the preprint in perpetuity. It is made available under aCC-BY 4.0 International license.

We have previously shown that inactivating *perRA* led to the derepression of *katE*, *ahpC* and *ccp* and to a higher tolerance to H_2O_2 [27,30] (see S2 Fig). The *perRA* mutant exhibited a reduced ability to grow in the presence of the superoxide-generating compound paraquat [30]. A mutant with a transposon inserted into the PerRB-encoding LIMLP_05620 ORF was available in our random transposon mutant library and was used to investigate *L. interrogans* tolerance of ROS in the absence of PerRB. When cultivated in EMJH medium, the *perRB* mutant did not reach the same density than the WT strain at stationary phase (Fig 5A and S2 Fig). Inactivating *perRB* did not have any effect on the ability of *L. interrogans* to tolerate deadly concentration of H_2O_2 (S2 Fig); however, it increases the capability of *Leptospira* to grow in the presence of paraquat (Fig 5B). Complementing in trans the *perRB* mutant restored the WT strain phenotype in the absence of paraquat (Fig 5A) and it decreased the growth rate of the cells to a somehow lower level than that of the WT in the presence of paraquat (Fig 5B). This indicates that PerRB is involved in *Leptospira* tolerance to superoxide, very likely by repressing (directly or indirectly) defenses against this ROS. Therefore, PerRA and PerRB have distinct function in pathogenic *Leptospira* survival in the presence of oxidants.

Identification of differentially-expressed genes upon *perRB* inactivation.

To understand the role of PerRB in *L. interrogans* tolerance to ROS, we compared the global transcriptional profiles of the *perRB* mutant and WT strains. Differential gene expression analysis revealed changes in the transcription of 123 genes, with 59 and 64 down- and up-regulated, respectively (see S2 Table for a complete set of data). However, *perRB* inactivation did not lead to dramatic changes in gene expression as the majority of Log_2FC (108 out of 123) ranged between -1 and 1 (S2 Table). These findings indicate that the absence of an active PerRB did not lead to substantial significant changes in genes expression when

bioRxiv preprint doi: https://doi.org/10.1101/2020.11.06.371039; this version posted November 6, 2020. The copyright holder for this preprint (which was not certified by peer review) is the author/funder, who has granted bioRxiv a license to display the preprint in perpetuity. It is made available under aCC-BY 4.0 International license.

280 *Leptospira* are cultivated in the laboratory conditions (in EMJH medium at 30°C) and during
281 the exponential phase.
282 Nevertheless, when examining the nature of the highest differentially-expressed genes in the
283 *perRB* mutant, some tendencies could be observed. Many of the differentially-expressed
284 ORFs were annotated as protein with unknown function and did not have homologs in the
285 saprophyte *L. biflexa* strain (S2 Table and Table 1).

ORF ID[a]	Gene	*L. biflexa*[b]	Function	Log2FC	Adjusted p-value
Down-regulated genes					
LIMLP_02490* (LIC12988/LA0587)		*LEPBI_I0886*	Lipase putative extracellular lipoprotein	-1.608	6.11e-04
LIMLP_02845 (LIC12920)			Hypothetical	-1.084	3.46e-02
LIMLP_03640** (LIC12763/LA0865)			Hypothetical	-1.102	1.06e-02
LIMLP_03790* (LIC12736/LA0905)			Hypothetical	-1.244	1.42e-05
LIMLP_04255 (LIC10892/LA3244)	*exbB*	LEPBI_I0149	Biopolymer transport protein ExbB/TolQ	-0.947	1.07e-02
LIMLP_06190** (LIC11265/LA2751)		LEPBI_I3113	Disulfide oxidoreductase	-0.723	6.96e-03
LIMLP_11400** (LIC12297/LA1456)	*radC*		DNA repair protein RadC	-0.619	1.17e-02
LIMLP_13165** (LIC12631/LA1029)	*sph2*		Sphingomyelinase C	-1.152	8.10e-03
LIMLP_14595* (LIC10628/LA3571)		LEPBI_I2694	Cytochrome oxidase CcoP subunit	-0.583	3.40e-02
LIMLP_14715** (LIC10606/LA3598)	*dps*	*LEPBI_I2540*	DNA-binding stress protein Dps	-0.896	1.61e-03
LIMLP_15470 (LIC10454/LA3793)**		LEPBI_I0671	Hemolysin (N-acyltransferase domain)	-1.317	3.40e-03
LIMLP_15890 (LIC10377/LA0430)			Hypothetical putative lipoprotein	-1.353	3.90e-10
LIMLP_16695 (LEPIC3326/LA4096)			Hypothetical	-1.124	8.14e-04
LIMLP_18235 (LIC20078/LB099)**			Hypothetical	-1.098	1.69e-02
Up-regulated genes					
LIMLP_02880* (LIC12912/LA0688)	*cas5*		CRISPR-associated protein Cas5	0.881	5.84e-03
LIMLP_02885* (LIC12911-12910/LA0689-0690)	*cas3*		CRISPR-associated protein Cas3	0.834	4.51e-03
LIMLP_04075** (LIC12680/LA0974)			Adhesin/FimH-like protein/DuF1566 domain	1.110	4.29e-03
LIMLP_05450* (LIC11125/LA2933)			Diguanylate cyclase	0.983	2.12e-04
LIMLP_05455* (LIC11126/LA2932)			Diguanylate cyclase	0.757	1.81e-02
LIMLP_05460* (LIC11127/LA2930)			Diguanylate cyclase	0.922	1.11e-03
LIMLP_05480 (LA2928)			Hypothetical	0.968	2.67e-02
LIMLP_05485** (LIC11131/LA2926)			Diguanylate cyclase	0.679	8.14e-04
LIMLP_05845 (LIC11203/LA2827)			Diguanylate phosphodiesterase	0.608	3.85e-02
LIMLP_09580 (LIC11921/LA1980)		LEPBI_I1269	Diguanylate phosphodiesterase	0.547	1.61e-02
LIMLP_17875 (LIC20015/LB017)	*hemN*	*LEPBI_I1166*	Coproporphyrinogen III oxidase HemN	0.727	9.53e-03
LIMLP_18375** (LIC20106/LB133)			Diguanylate phosphodiesterase	0.593	1.99e-02
LIMLP_18755 (LIC20176/LB225)			Hypothetical putative lipoprotein	1.453	3.77e-04
LIMLP_18760 (LIC20177/LB226)			Adhesin/FimH-like protein/ DUF1566 domain-containing protein	1.095	3.39e-02
LIMLP_19320* (LA1770)			AraC family transcriptional regulator	1.279	4.51e-03
LIMLP_19325* (LA1771)			Hypothetical	1.262	4.05e-02

Table 1. Differentially-expressed ORFs upon *perRB* inactivation

Selected up-and down-regulated genes in the LIMLP_05620 (*perRB*) mutant with an adjusted p-value cutoff of 0.05.

[a] Gene numbering is according to Satou *et al* [31]. Corresponding genes of *L. interrogans* serovar Lai strain 56601 and serovar Copenhageni Fiocruz strain L1-130 are indicated in parenthesis.

[b] Closest ortholog in the saprophytes *L. biflexa* serovar Patoc strain Patoc1. The absence of syntheny is indicated in italic.

Genes that are down-regulated upon *perRA* inactivation as determined previously [27] are indicated in bold.

Down (*) and up (**) -regulated genes upon exposure to lethal H_2O_2 dose as determined previously [27].

bioRxiv preprint doi: https://doi.org/10.1101/2020.11.06.371039; this version posted November 6, 2020. The copyright holder for this preprint (which was not certified by peer review) is the author/funder, who has granted bioRxiv a license to display the preprint in perpetuity. It is made available under aCC-BY 4.0 International license.

Among the highest up-regulated genes, two ORFs (LIMLP_04075 and LIMLP_18760) encoded lipoproteins with a putative adhesin function. These proteins contain DUF1566 domain repeats which is also share by Lsa25, a Leptospiral surface adhesin that binds extracellular matrix (ECM) [32].

Several genes involved in the metabolism of c-di GMP were differentially-expressed upon *perRB* inactivation. C-di GMP is a secondary messenger in bacteria that regulates a variety of processes such as biofilm formation, motility, stress adaptation, and virulence. C-di GMP synthesis is catalyzed by diguanylate cyclases (DGCs) whereas its hydrolysis is catalyzed by phosphodiesterases (PDEs). DGCs and PDEs are numerous in pathogenic *Leptospira*, suggesting that c-di GMP fulfills an important role in sensing environmental signals when *Leptospira* infect and colonize a host. C-di GMP has been recently shown to regulate biofilm formation, motility and protection against environmental stress in pathogenic *Leptospira* [33]. Four DGCs (LIMLP_05450, LIMLP_05455, LIMLP_05460, LIMLP_05485) were up-regulated upon *perRB* inactivation (Table 1). These DGC-encoding ORFs are located in a gene cluster (LIMLP_05485-05450) that contains 7 ORFs coding for DGCs. LIMLP_05450, LIMLP_05455, LIMLP_05460, and LIMLP_05485 display the typical diguanylate cyclase GGDEF and sensory PAS domains. A DGC activity was demonstrated *in vitro* for LIMLP_05450, LIMLP_05455, LIMLP_05460 [34]. Three PDE-encoding ORFs (LIMLP_05845, LIMLP_9580, and LIMLP_18375) were also up-regulated in the *perRB* mutant.

LIMLP_13165 was among the most down-regulated ORFs when *perRB* was inactivated. It encodes a secreted protein with sphingomyelinase C and hemolytic activities [35]. Another significantly down-regulated ORF encoded a protein with an acyl CoA acetyl tranferase domain annotated as a putative hemolysin (LIMLP_15470). This ORF is up-regulated when *L. interrogans* is cultivated in DMC implemented in rats [36].

bioRxiv preprint doi: https://doi.org/10.1101/2020.11.06.371039; this version posted November 6, 2020. The copyright holder for this preprint (which was not certified by peer review) is the author/funder, who has granted bioRxiv a license to display the preprint in perpetuity. It is made available under aCC-BY 4.0 International license.

An ORF encoding an AraC transcriptional regulator (LIMLP_19320), and two ORFs of unknown function (LIMLP_18755 and 19325) were among the most up-regulated. The orthologs of LIMLP_19320 and LIMLP_19325 in *L. interrogans* serovar Lai belongs to a genomic island (Lai GI B, LA1747-1851) that can excise from the chromosome and form an independent replicative plasmid [37,38].

Among the down-regulated genes, several ORFs encode factors related to oxidative stress. LIMLP_04255 is part of a gene cluster (LIMLP_04240-04285) which code for a putative TonB-dependent transport system repressed by PerRA. We have previously shown that some genes of this cluster (LIMLP_04245, LIMLP_04270 and LIMLP_04280) are involved in *L. interrogans* tolerance to superoxide [27]. LIMLP_11400 encodes the DNA repair protein RadC and LIMLP_14715 is a homolog of the *E. coli* Dps, a protein that sequesters iron and protects DNA from oxidative damage. LIMLP_06190 encodes a putative disulfide oxidoreductase with the N-terminal ScdA domain (DUF1858). In *S. aureus*, ScdA is a di-iron protein involved in repair of oxidatively damaged iron-sulfur cluster proteins [39]. LIMLP_14595 encodes a putative transmembrane lipoprotein with a cytochrome-like domain that shows homology with the CcoP subunit of the cytochrome C oxidase and could function in the respiratory chain or be an enzyme cofactor.

Only 7 out of the 123 differentially-expressed genes in the *perRB* mutant were also differentially-expressed upon *perRA* inactivation with a similar inclination (S3 Fig) [27]. LIMLP_02010 and LIMLP_04325 were up-regulated whereas LIMLP_04255, LIMLP_11810, LIMLP_14225, LIMLP_15470 and LIMLP_18235 were down-regulated in the two mutants.

Notably, 82 out of the 123 differentially-expressed ORFs in the *perRB* mutant were also differentially-expressed upon exposure of *L. interrogans* to H_2O_2 (S3 Fig) [27]. Thus, 66% of the PerRB regulon is also regulated by the presence of H_2O_2. Interestingly, the majority of

bioRxiv preprint doi: https://doi.org/10.1101/2020.11.06.371039; this version posted November 6, 2020. The copyright holder for this preprint (which was not certified by peer review) is the author/funder, who has granted bioRxiv a license to display the preprint in perpetuity. It is made available under aCC-BY 4.0 International license.

345 ORFs down-regulated in the *perRB* mutant, including the RadC and the Dps-encoding ORFs,
346 were up-regulated in the presence of H_2O_2 (with Log_2FCs of 3.46 and 1.10, respectively) (S3
347 Fig and Table 1). On the contrary, many up-regulated ORFs in the *perRB* mutant had a lower
348 expression in the presence of H_2O_2. For instance, the ORFs that code for Cas5
349 (LIMLP_02880), Cas3 (LIMLP_02885), and two DGCs (LIMLP_05450 and LIMLP_05455)
350 were down-regulated upon exposure to H_2O_2 with Log_2FCs lower than -1.21 (S3 Fig and
351 Table 1).
352
353 **Concomitant inactivation of *perRA* and *perRB* leads to a higher resistance to ROS but to**
354 **a lower virulence**
355 In order to investigate whether PerRA and PerRB cooperate in regulating the adaptive
356 response to ROS, we inactivated *perRA* by allelic exchange in the *perRB* mutant (S4 Fig).
357 This allowed obtaining a double *perRAperRB* mutant in a *L. interrogans* strain, the first
358 double mutant constructed in a pathogenic *Leptospira*.
359 The double *perRAperRB* mutant had a growth rate comparable to that of the single *perRA* and
360 *perRB* mutants and WT strains when *L. interrogans* were cultivated in EMJH medium (Fig
361 6A). However, entry in exponential phase was delayed if the culture medium was inoculated
362 with stationary phase-adapted *perRAperRB* mutant (S5 Fig). We had already shown that a
363 *perRA* mutant had a higher ability to grow and survive in the presence of deadly concentration
364 of H_2O_2 but a slower growth in the presence of the superoxide-generating paraquat ([30], and
365 see in S2 Fig and Figs 6B and 6C). On the contrary, inactivating *perRB* leads to a higher
366 resistance to paraquat (Fig 5 and Fig 6C). The concomitant inactivation of *perRA* and *perRB*
367 led to a greater growth in the presence of both H_2O_2 (Fig 6B) and paraquat (Fig 6C). To
368 complement the double *perRAperRB* mutant strain, the PerRB-encoding ORF LIMLP_05620
369 was expressed in trans using the replicative pMaORIgenta vector (S4 Fig). The growth of the

bioRxiv preprint doi: https://doi.org/10.1101/2020.11.06.371039; this version posted November 6, 2020. The copyright holder for this preprint (which was not certified by peer review) is the author/funder, who has granted bioRxiv a license to display the preprint in perpetuity. It is made available under aCC-BY 4.0 International license.

370 trans-complemented *perRAperRB* mutant resumed to an impaired growth, as that of the WT
371 and single *perRA* mutant strains, in the presence of paraquat (Fig 6D). Therefore, the double
372 *perRAperRB* mutant exhibited cumulative phenotypes of the respective single *perRA* and
373 *perRB* mutants when *L. interrogans* are cultivated in the presence of ROS.
374 We then tested whether *perRA* and *perRB* inactivation had any influence on *L. interrogans*
375 virulence in the animal model of acute leptospirosis. All hamsters infected intraperitoneally
376 with 10^4 bacteria of the *perRA* or *perRB* single mutant strains exhibited morbidity sign after
377 7-8 days (Fig 6E), similarly to the WT strain. In contrast, all animals infected
378 intraperitoneally with 10^4 bacteria of the double *perRAperRB* mutant strain did not show any
379 sign of morbidity three weeks post-infection (Fig 6E), even when the animals were infected
380 with 10^6 bacteria of the double *perRAperRB* mutant strain (Fig 6F). Virulence was restored in
381 the double *perRAperRB* mutant strain complemented in trans only with *perRB* (Fig 6F).
382 Therefore, the concomitant inactivation of *perRA* and *perRB* resulted in a loss of virulence in
383 *L. interrogans* and expressing only *perRB* in the double mutant restored *Leptospira* virulence.
384 Altogether, these results demonstrate that despite a higher resistance to ROS, the double
385 *perRAperRB* mutant exhibited a dramatically reduced virulence.
386

387 **Concomitant inactivation of *perRA* and *perRB* has a pleiotropic effect in *L.***
388 ***interrogans* gene expression.**

389 To further understand the interplay between PerRA and PerRB in controlling the
390 oxidative stress response and virulence in *L. interrogans*, we performed RNA-Seq
391 experiments on the double *perRAperRB* mutant and compared its transcriptomic profile with
392 that of WT and single *perRA* and *perRB* mutant strains.
393 949 and 1024 ORFs were down- and up-regulated, respectively, in the double
394 *perRAperRB* mutant (Fig 7A and see S3 Table for a complete set of data). Therefore,

bioRxiv preprint doi: https://doi.org/10.1101/2020.11.06.371039; this version posted November 6, 2020. The copyright holder for this preprint (which was not certified by peer review) is the author/funder, who has granted bioRxiv a license to display the preprint in perpetuity. It is made available under aCC-BY 4.0 International license.

concomitant *perRA* and *perRB* inactivation resulted in differential expression of almost half of the total coding sequences of *L. interrogans*; in comparison, only about 1% and 3% of the total coding sequences of *L. interrogans* were differentially-expressed in the single *perRA* and *perRB* mutants, respectively (S2 Table) [27]. Volcano scatter plot representation indicated not only a higher magnitude of fold changes but also a greater statistical significance in the double *perRAperRB* mutant (Fig 7B-D).

Most of the differentially-expressed ORFs in the *perRA* mutant were also differentially-expressed in the double *perRAperRB* mutant (Fig 7A). Many genes of the LIMLP_04240-04280 cluster encoding a putative TonB-dependent transport system, the two-component system VicKR (LIMLP_16720-16725), a putative hemolysin (LIMLP_15470) and several ORFs of unknown function (from LIMLP_14190 to LIMLP_14225) were down-regulated in the *perRA* [24,27] and *perRAperRB* mutants (Fig 7 and 8A, S4 Table). Likewise, the ORFs encoding the catalase, AhpC and CCP (LIMLP_10145, LIMLP_05955 and LIMLP_02795, respectively), that are repressed by PerRA and up-regulated in the single *perRA* mutant [24,27], were also up-regulated in the double *perRAperRB* mutant (Fig 7 and 8B, S5 Table).

21 and 27 ORFs that are respectively down- and up-regulated in the *perRB* mutant were also down- and up-regulated in the *perRAperRB* mutant (Fig 7A). LIMLP_11400 (encoding RadC), LIMLP_04255, encoding ExbB of the TonB-dependent transport system, the hemolysin-encoding ORF LIMLP_15470, and LIMLP_15890 were down-regulated in the single *perRB* and double *perRAperRB* mutants (Fig 7 and S2-S4 Tables).

Interestingly, the vast majority of the differentially-expressed ORFs in the double *perRAperRB* mutant did not exhibit any change in their expression in the single *perRA* and *perRB* mutants. For instance, of the DGCs and PDEs that were up-regulated in the *perRB* mutant, only LIMLP_09580 was up-regulated in the double *perRAperRB* mutant (S2, S3 and S5 Tables). In fact, the *perRAperRB* double mutant exhibited a distinct expression pattern of

bioRxiv preprint doi: https://doi.org/10.1101/2020.11.06.371039; this version posted November 6, 2020. The copyright holder for this preprint (which was not certified by peer review) is the author/funder, who has granted bioRxiv a license to display the preprint in perpetuity. It is made available under aCC-BY 4.0 International license.

genes involved in signaling (Fig 8C). The LIMLP_07050 ORF that codes for a DGC was down-regulated; two ORFs encoding adenylate/guanylate cyclases (LIMLP_00130 and LIMLP_02085) and the PDE-encoding LIMLP_04775 ORF were up-regulated in the *perRAperRB* mutant. Finally, only 6 ORFs were differentially expressed in all mutants (Fig 7A), including LIMLP_04255 and LIMLP_15470 (S4 and S5 Tables). Moreover, a substantial number of regulatory factors (transcriptional regulators, two-component systems, sigma factors) were differentially-expressed exclusively in the *perRAperRB* mutant (S4 and S5 Tables).

In the double *perRAperRB* mutant, several ORFs encoding factors putatively involved in cell growth (cell division, respiration and cell wall homeostasis), chemotaxis and motility are significantly up-regulated, with a Log_2FC greater than 1.5 (S5 Table). This correlates with a higher ability of the *perRAperRB* mutant to reach a higher cell number when cultivated *in vitro* at 30°C (Fig 6 and S4 Fig).

In addition to the PerRA-repressed peroxidases (catalase, AhpC, CCP), other oxidative-stress related factors exhibited a higher expression in the *perRAperRB* mutant (Fig 8B). DoxX-encoding ORF, which is up-regulated upon concomitant *perRA* and *perRB* inactivation (Log_2FC 1.65), is an integral membrane protein that interacts with SodA in *M. tuberculosis* and participates in tolerance to oxidative and redox stress [40]. Two imelysins (LIMLP_14170/LruB and LIML_14180) and a thiol peroxidase (LIML_14175) exhibited also a higher expression in the *perRAperRB* mutant (Log_2FC of 2.36, 1.93, and 2.04 respectively, Fig 8B). All these up-regulated factors (except DoxX) were also up-regulated upon exposure to deadly H_2O_2 dose [27] and they probably participate in the higher tolerance of the double mutant in the presence of oxidants. Despite the up-regulation of several factors involved in the defense against ROS, the DNA repair protein RadC (encoded by LIMLP_11400) and the

bioRxiv preprint doi: https://doi.org/10.1101/2020.11.06.371039; this version posted November 6, 2020. The copyright holder for this preprint (which was not certified by peer review) is the author/funder, who has granted bioRxiv a license to display the preprint in perpetuity. It is made available under aCC-BY 4.0 International license.

glutathione S transferase (encoded by LIMLP_13670) were notably down-regulated in the *perRAperRB* mutant (Log2FC of -1.9 and -2.3, respectively) (Fig 8B and S4 Table).

Strikingly, several down-regulated ORFs in the double *perRAperRB* mutant such as *clpB*, *ligA*, *ligB*, and the operon *lvrAB* have been associated with *Leptospira* virulence. As in many bacteria, leptospiral ClpB ATPase is involved in disaggregating protein aggregates arising upon stress-induced protein denaturation [41]. *ClpB* expression is increased upon exposure to H_2O_2 and it is required for *Leptospira* virulence [27,42]. The ClpB-encoding ORF (LIMLP_10060) is dramatically down-regulated in the *perRAperRB* mutant (Log_2FC of -2.99) (Fig 8D and S4 Table).

Another virulence factors in *Leptospira* are the immunoglobulin-like LigA (LIMLP_15405) and LigB (LIMLP_15415) proteins. These surface-exposed proteins are involved in adhesion to host cells through ECM binding [43] and participate in the immune evasion through binding to the host complement Factor H and C4b binding protein [44]. Simultaneous down-regulation of *ligA* and *ligB* expression led to attenuation of *Leptospira* virulence [45]. *LigA* and *ligB* were down-regulated in the *perRAperRB* mutant (Log2FC of -3 and -2.44, respectively) (Fig 8D and S5 Table).

LvrA (LIMLP_08490) and *lvrB* (LIMLP_08485) encode a hybrid histidine kinase and a hybrid response regulator, respectively. Inactivation of the *lvrAB* operon led to virulence attenuation in *L. interrogans* [46]. *LvrA* and *lvrB* had both a decreased expression in the *perRAperRB* mutant (Log2FC of -2.3) (Fig 8D and S5 Table).

Additional ORFs encoding chaperones (the small heat shock proteins Hsp15 and Hsp20) or enzymes involved in protein folding (the disulfide isomerase DsbD and the peptidyl-prolyl cis-trans isomerase SlyD) and degradation (HtpX) were down-regulated in the *perRAperRB* mutant. The involvement of these factors in *Leptospira* virulence has not been demonstrated but small Hsps participate in *M. tuberculosis* growth in macrophages [47]. DsbD and these

bioRxiv preprint doi: https://doi.org/10.1101/2020.11.06.371039; this version posted November 6, 2020. The copyright holder for this preprint (which was not certified by peer review) is the author/funder, who has granted bioRxiv a license to display the preprint in perpetuity. It is made available under aCC-BY 4.0 International license.

two small Hsps were up-regulated in *L. interrogans* upon exposure to H_2O_2 [27]. All these factors might protect *Leptospira* proteostasis under adverse conditions as encountered during infection inside a host. The down-regulation of these virulence-associated genes together with the differential expression of several other genes was confirmed by RT-qPCR (S5 Fig). Interestingly, gene expression of the virulence-associated genes (*lvrA*, *lvrB*, *ligA*, *ligB*, *clpB*, *hsp15*, and *hsp20*) was increased to the WT level (or even to a higher level) in the double *perRAperRB* mutant strain complemented in trans only with *perRB* (Fig 9).

Taken together, these findings indicate that the loss of virulence resulting from the concomitant inactivation of *perRA* and *perRB* correlated with a global deregulation of a complex gene network, including genes associated with virulence.

Identification of differentially-expressed non-coding RNAs in the *perRB* and *perRAperRB* mutants.

Intergenic regions were also analyzed to identify differentially expressed predicted non-coding RNAs (ncRNAs). As observed for coding sequences, inactivation of *perRB* led to the deregulation of only a few putative ncRNAs and most of the changes in expression were below two folds (see S6 Table for a complete set of data). Nonetheless, a few numbers of ncRNAs were significantly down-regulated with a Log_2FC below -1 (S7 Table). Some of the differentially-expressed ncRNAs (LepncRNA36, LepncRNA87, LepncRNA89, LepncRNA109, LepncRNA139) were located in the proximate vicinity of differentially-expressed ORFs in the *perRB* mutant. Three ncRNAs (LepncRNA35, LepncRNA89 and LepncRNA109) were also differentially expressed upon *perRA* inactivation (S7 Table) [27].

55 putative ncRNAs were differentially-expressed (with a Log_2FC cutoff of ±1) in the *perRAperRB* mutant and several of them were adjacent or overlapped differentially-expressed

bioRxiv preprint doi: https://doi.org/10.1101/2020.11.06.371039; this version posted November 6, 2020. The copyright holder for this preprint (which was not certified by peer review) is the author/funder, who has granted bioRxiv a license to display the preprint in perpetuity. It is made available under aCC-BY 4.0 International license.

493 ORFs (S8 Table). Only a few of these differentially-expressed ncRNAs had an altered
494 expression in the single *perRA* and *perRB* mutant (S8 Table) [27].
495 Among the most highly differentially-expressed ncRNAs was LepncRNA38 that was located
496 downstream *ccp*, a highly up-regulated ORF in the *perRAperRB* mutant (Fig 10 and S8
497 Table). LepncRNA38 and *ccp* were also up-regulated in the *perRA* mutant [27]. The ncRNA
498 LepncRNA49, which was down-regulated in the *perRAperRB* mutant, overlapped with *exbB*
499 (LIMLP_04255), an ORF that was also down-regulated in the double *perRAperRB* mutant as
500 well as in the single *perRA* and *perRB* mutants (Fig 10). The down-regulated LepncRNA105
501 and LepncRNA130 ncRNAs were located downstream the *hsp20-15* operon and *gst*,
502 respectively, three ORFs whose expression is decreased is the *perRAperRB* mutant (Fig 10
503 and S8 Table). It is worth noting that LepncRNA38, LepncRNA105 and LepncRNA130 are
504 up-regulated by H_2O_2 as were *ccp*, *hsp20-15* and *gst* ([27]; Fig 10).
505 Altogether, these findings indicate that the absence of both PerRA and perRB triggers major
506 changes in the transcriptional activity of many ncRNAs in *L. interrogans*, that could
507 consequently alter the expression of many ORFs.
508
509

bioRxiv preprint doi: https://doi.org/10.1101/2020.11.06.371039; this version posted November 6, 2020. The copyright holder for this preprint (which was not certified by peer review) is the author/funder, who has granted bioRxiv a license to display the preprint in perpetuity. It is made available under aCC-BY 4.0 International license.

Discussion

Virulence mechanisms are poorly characterized in pathogenic *Leptospira*. These bacteria possess a high number of genes encoding proteins of unknown function (40% of the genomes) and many of them are pathogen-specific. Pathogenic *Leptospira* spp. lack many classical virulence factors, such as a type III to type VI secretion systems, and it is unclear which factors are important for its pathogenesis. It is therefore generally agreed that these pathogens possess unique virulence factors. Nonetheless, studying heme oxygenase and catalase mutants have shown that, *in vivo*, iron acquisition and defense against peroxide stress are important virulence-associated mechanisms in *L. interrogans* [11,48]. Catalase is repressed by PerRA [24,27] and genes encoding factors involved in iron uptake are very likely controlled by regulators of the Fur-family.

In addition to PerRA, pathogenic *Leptospira* contain three other ORFs annotated as Furs. In the present study, we have characterized the *L. interrogans* Fur-like regulator encoded by LIMLP_05620 and showed that it exhibits characteristic features of a PerR regulator. We consequently named this ORF *perRB*. Sequence alignment and phylogenetic analyses revealed that PerRB is the closest relative to the already characterized PerRA, and perhaps more importantly, they both do exhibit the canonical amino acid residues that are the hallmark of a PerR. The H_2O_2 sensing histidine and aspartate residues are conserved in *Leptospira* PerRA and PerRB and, interestingly, both genes are H_2O_2-responsive, albeit with different apparent sensitivity. This is consistent with a mechanism whereby PerRA and PerRB would repress their own transcription and dissociate from their promoter upon oxidation by H_2O_2, leading to alleviation of repression. Moreover, the higher survival of the *perRB* mutant in the presence of superoxide suggests a derepression of genes encoding defenses against ROS and therefore the participation of PerRB in controlling the adaptation to oxidative stress. Neither

bioRxiv preprint doi: https://doi.org/10.1101/2020.11.06.371039; this version posted November 6, 2020. The copyright holder for this preprint (which was not certified by peer review) is the author/funder, who has granted bioRxiv a license to display the preprint in perpetuity. It is made available under aCC-BY 4.0 International license.

535 *perRA* nor *perRB* expression was up-regulated in iron-limiting condition [24]. Although the
536 putative lipoprotein LIMLP_18755 was significantly up-regulated in the *perRB* mutant and
537 under iron-limiting condition, there was no strong overlap between PerRB regulon and the
538 transcriptional response to iron-limiting condition [24]. Altogether, these findings could argue
539 in favor of LIMLP_05620 encoding a PerR-like regulator rather than a Fur. However, because
540 iron homeostasis and oxidative stress are intertwined, a certain functional relationship has
541 been observed between PerR and Fur. In several bacteria where PerR and Fur coexist,
542 including *B. subtilis* and *C. jejuni*, the PerR regulon overlaps with that of Fur [49,50]. In
543 addition, *fur* and several Fur-regulated genes are also differentially expressed in the presence
544 of H_2O_2 [51,52]. In fact, PerR represses *fur*, whose expression is up-regulated in the presence
545 of H_2O_2 as a consequence of dissociation of PerR from the *fur* promotor [53,54]. Metal-
546 catalyzed oxidation of the H_2O_2 sensing residues will be fundamental in establishing that the
547 Per-like regulator encoded by LIMLP_05620 is a *bona fide* PerR.
548 To the best of our knowledge, this is the first report that has identified the coexistence of two
549 PerR regulators in a pathogenic Gram-negative bacterium. The coexistence of three PerR-like
550 regulators has been reported only in Gram-positive bacteria such as *B. licheniformis* and *M.*
551 *smegmatis*. It was shown that the three *B. licheniformis* PerRs sense hydrogen peroxide by
552 histidine oxidation, although with different sensitivity [55] . In *M. smegmatis*, three Fur-like
553 paralogs displayed the canonical PerR Asp residue involved in H_2O_2 sensitivity, exhibited
554 H_2O_2 sensing by metal-catalyzed histidine oxidation and a higher H_2O_2 resistance when their
555 genes were inactivated [56].
556 One important question was to understand the mechanism that have led to the coexistence of
557 PerRA and PerRB exclusively in highly virulent species (P1 clade). Virulent mammalian-
558 adapted strains in the *Leptospira* genus might have originated from a free-living ancestor
559 inhabiting soils. The phylogenetic analysis presented here indicates that the coexistence of

bioRxiv preprint doi: https://doi.org/10.1101/2020.11.06.371039; this version posted November 6, 2020. The copyright holder for this preprint (which was not certified by peer review) is the author/funder, who has granted bioRxiv a license to display the preprint in perpetuity. It is made available under aCC-BY 4.0 International license.

PerRA and PerRB is not due to gene duplication. Indeed, PerRA was already present in the leptospirales ancestor whereas PerRB was probably acquired by pathogenic species by horizontal transfer from a soil/aquatic bacterium of another phylum. In this scenario, PerRA would had been lost by the P2 clade intermediate species but maintained together with PerRB by the P1 clade species to establish full virulence.

We had previously shown that when *perRA* was inactivated, *L. interrogans* acquired a higher resistance to H_2O_2 explained by the derepression of *katE*, *ahpC* and *ccp* [24,27]. Here, we have demonstrated that inactivating *perRB* resulted in a higher survival of *L. interrogans* in the presence of the superoxide but it did not affect the survival of *L. interrogans* in the presence of H_2O_2. Therefore, even though *perRB* is up-regulated upon exposure to H_2O_2 as *perRA*, the consequence of *perRB* inactivation is different than that of *perRA*, suggesting that PerRA and PerRB have a distinct and non-redundant function in *Leptospira* adaptation to oxidative stress. The distinct repartition of PerRA and PerRB in the *Leptospira* genus and differences in their respective regulon support the hypothesis of a non-redundant function in the adaptation to oxidative stress. The PerRA and PerRB regulons determined when *L. interrogans* are cultivated inside a host using DMC implemented in rats confirmed the limited overlap between PerRA and PerRB regulons [57].

Phenotypic studies suggest that PerRB represses (directly or indirectly) genes encoding defenses against superoxide. Highly pathogenic *Leptospira* species (from the P1 clade) do not encode any SOD or SOR that could be responsible for detoxification of superoxide whereas intermediated species (P2 clade) and saprophyte non-pathogenic *Leptospira* do have such enzymes. Understanding how pathogenic *Leptospira* detoxify superoxide encountered during infection is a very important question. Overall, the differentially-expressed genes upon *perRB* inactivation are mostly *Leptospira*-specific and poorly characterized. Examining the PerRB regulon determined when *Leptospira* are cultivated in laboratory conditions did not allow to

bioRxiv preprint doi: https://doi.org/10.1101/2020.11.06.371039; this version posted November 6, 2020. The copyright holder for this preprint (which was not certified by peer review) is the author/funder, who has granted bioRxiv a license to display the preprint in perpetuity. It is made available under aCC-BY 4.0 International license.

585 draw a conclusive hypothesis on the identity of the factors that could participate in superoxide
586 detoxification in *L. interrogans*. The highest differentially-expressed ORFs were mainly
587 involved in regulation and cell signaling (transcription and sigma factors,
588 adenylate/diguanylate cyclase, TCSs) and could be involved in regulating the adaptation to
589 various challenging stress encountered in the environment or within a host. Further studies
590 will be required to determine whether superoxide detoxification in *L. interrogans* is mediated
591 by enzymatic detoxification or metal-dependent scavenging mechanisms and to clarify the
592 exact role of PerRB in controlling those pathways.
593 The low number of significantly differentially-expressed genes in the *perRB* mutant when *L.*
594 *interrogans* are cultivated *in vitro* led us to propose that PerRB exerts its function during
595 oxidative stress or upon host-related conditions. Consistent with this hypothesis is the up-
596 regulation of *perRB* in the presence of lethal H_2O_2 dose. It is worth noting that there is, to
597 some extent, an overlap between the PerRB regulon and the differentially-expressed genes
598 upon exposure to lethal H_2O_2 dose [27]. Moreover, the exclusive presence of PerRB in the
599 pathogenic *Leptospira* clades strongly suggests that PerRB function is more related to
600 regulating adaptation to infection-related conditions rather than to environmental survival.
601 Very interestingly, when the *perRB* mutant was cultivated in the host conditions using the
602 DMC implants, a higher number of genes were differentially-expressed with greater fold
603 changes than when the *perRB* mutant was cultivated at 30°C in the laboratory conditions [57].
604 Notably, in the host condition, the absence of *perRB* also led to the deregulation of several
605 genes involved in signaling and regulation, which is consistent with a role of PerRB in
606 regulating adaptation to the host environment [57].
607 One feature of *Leptospira* genus is the genetic and functional redundancy where multiple
608 genes commonly encode for a similar function. The development of genetic tools has made
609 random and targeted mutagenesis possible, albeit with a low efficiency. Due to this limitation,

bioRxiv preprint doi: https://doi.org/10.1101/2020.11.06.371039; this version posted November 6, 2020. The copyright holder for this preprint (which was not certified by peer review) is the author/funder, who has granted bioRxiv a license to display the preprint in perpetuity. It is made available under aCC-BY 4.0 International license.

610 only a few *Leptospira* virulence factors have been identified and have fulfilled Koch's
611 molecular postulates. The present study is the first to report the concomitant inactivation of
612 two genes and complementation of a double mutant in a pathogenic *Leptospira*. Obtaining a
613 double *perRAperRB* mutant gave us the unique opportunity to investigate the functional
614 relationship between two PerR-like regulators in a pathogenic bacterium.
615 In many pathogens which contain only one PerR paralog, such as *N. gonorrhoeae*, *S.*
616 *pyogenes,* and *S. aureus*, PerR was shown to be involved in virulence [54,58–61]. The single
617 *L. interrogans perRA* and *perRB* mutants still retain full virulence in the model for acute
618 leptospirosis (this study and [24]). Interestingly, virulence attenuation was only observed
619 upon the concomitant inactivation of *perRA* and *perRB*, suggesting an interplay in controlling
620 (directly or indirectly) *L. interrogans* virulence-associated genes. The loss of virulence
621 correlated with a large differential gene and ncRNA expression compared not only with the
622 WT but also with the single mutant strains. In other words, the double *perRAperRB* displayed
623 differential gene expression that were not observed in the single *perRA* and *perRB* mutants.
624 This could indicate that a subset of genes and ncRNAs is controlled by both PerRA and
625 PerRB. The absence of one regulator could be compensated by the other and most of the
626 genes and ncRNAs that can be regulated by the two regulators would not be differentially
627 expressed in the single mutants. The few genes (LIMLP_02010, LIMLP_04255,
628 LIMLP_04235, LIMLP_11810, LIMLP_14225, LILP_15470, and LIMLP_18235) and
629 ncRNAs that display differential expression in the single mutants in our transcriptomic
630 studies (this study and [27]) indicate a certain functional redundancy of the two regulators
631 even if the phenotypic analyses of the mutants suggest distinct functions. The change in
632 expression of a few regulators when PerRA and PerRB are both absent could lead to major
633 changes in expression of many ORFs or ncRNAs in cascade. One can also speculate that
634 among the large differentially-expressed genes only observed in the double *perRAperRB*

bioRxiv preprint doi: https://doi.org/10.1101/2020.11.06.371039; this version posted November 6, 2020. The copyright holder for this preprint (which was not certified by peer review) is the author/funder, who has granted bioRxiv a license to display the preprint in perpetuity. It is made available under aCC-BY 4.0 International license.

635 mutant some deregulation might be due to a compensatory effect to maintain a productive
636 fitness.
637 Despite a higher ability to resist ROS, the double *perRAperRB* mutant has lost its virulence; it
638 could not trigger acute leptospirosis-associated morbidity. This could be obviously explained
639 by a significant lower expression of several virulence-associated factors in the double
640 *perRAperRB* mutant, such as LigA, LigB, LvrA, LvrB, and ClpB. In addition, other
641 dramatically down-regulated genes encode factors such as small Hsps (Hsp15 and Hsp20) for
642 which a role in bacterial virulence is demonstrated in other bacteria including *M. tuberculosis*
643 [62]. Moreover, several differentially-expressed ORFs of unknown function could also be
644 responsible for the loss of virulence of the double *perRAperRB* mutant. It is noteworthy that
645 the double *perRAperRB* mutant was also unable to colonize mice [57] and, consistent with
646 what is observed with *in vitro*-cultivated *perRAperRB* mutant, this correlated with dramatic
647 gene dysregulation including down-regulation of *ligA* and *ligB* [57].
648 In summary, this study has allowed to identify a second PerR-like regulator in pathogenic *L.*
649 *interrogans* strains that cooperates with PerRA to control the adaptation to oxidative stress
650 and virulence. By concomitantly inactivating *perRA* and *perRB* and establishing the molecular
651 Koch' postulates, we have unveiled a complex regulatory network that reveals, for the first
652 time, a functional relationship between PerR regulators and *Leptospira* virulence, most likely
653 through the regulation of virulence- and pathogenicity-associated factors.
654

bioRxiv preprint doi: https://doi.org/10.1101/2020.11.06.371039; this version posted November 6, 2020. The copyright holder for this preprint (which was not certified by peer review) is the author/funder, who has granted bioRxiv a license to display the preprint in perpetuity. It is made available under aCC-BY 4.0 International license.

Materials and Methods

Bacterial strains and growth condition

L. interrogans serovar Manilae strain L495, *perRA* (M776), *perRB* (M1474), and the double *perRAperRB* mutant strains (see S9 Table for a complete description of the strains used in this study) were grown aerobically at 30°C in Ellinghausen-McCullough-Johnson-Harris medium (EMJH) [63] with shaking at 100 rpm. *Leptospira* growth was followed by measuring the absorbance at 420 nm. β2163 and Π1 *E. coli* strains were cultivated at 37°C in Luria-Bertani medium with shaking at 37°C in the presence of 0.3 mM thymidine or diaminopimelic acid (Sigma-Aldrich), respectively. When needed, spectinomycin, kanamycin and gentamycin were added at the respective concentration of 50 µg/ml, 30 µg/ml, and 8 µg/ml.

Concomitant inactivation of *perRA* (LIMLP_10155) and *perRB* (LIMLP_05620).

PerRA gene (LIMLP_10155/LIC12034/LA1857) was inactivated in the *perRB* (LIMLP_05620/LIC11158/LA2887) mutant strain (M1474, *perRB::Km*^{R}) by introduction of a spectinomycin resistance cassette (S4 Fig). For this, a spectinomycin resistance cassette flanked by 0.8 kb sequences homologous to the sequences flanking *perRA* was created by gene synthesis (GeneArt, Life Technologies) and cloned into a kanamycin-resistant *Escherichia coli* vector unable to replicate in *Leptospira*. The obtained suicide plasmid (pKΔperRA) (S10 Table) was introduced in the *perRB* mutant strain by electroporation as previously described [64] using a Gene Pulser Xcell (Biorad). Individual spectinomycin-resistant colonies were selected on EMJH plates containing 50 µg/ml spectinomycin and screened by PCR (using the P1 and P2 primer set, see S11 Table) for proper replacement of the *perRA* coding sequence by the spectinomycin resistance cassette. *PerRA* inactivation in the double *perRAperRB* mutant was verified by western blot using an anti-PerRA serum (S4 Fig).

bioRxiv preprint doi: https://doi.org/10.1101/2020.11.06.371039; this version posted November 6, 2020. The copyright holder for this preprint (which was not certified by peer review) is the author/funder, who has granted bioRxiv a license to display the preprint in perpetuity. It is made available under aCC-BY 4.0 International license.

680

681 **Complementation of the single *perRB* and double *perRAperRB* mutants**

682 The *perRB* mutant *(perRB::Km^R)* complementation was performed by expressing the *perRB*
683 ORF in the pMaORI replicative vector [65]. The *perRB* (LIMLP_05620) ORF together with
684 its native promoter region (200 bp upstream region) were amplified from genomic DNA of *L.*
685 *interrogans* serovar Manilae strain L495 (using the ComPerR2_5Not and ComPerR2_3Xba
686 primer set, S11 Table) and cloned between the Not1 and Xba1 restriction sites in the pMaORI
687 vector. The absence of mutation in the *perRB* ORF in the obtained plasmid (pNB139) was
688 checked by DNA sequencing and the pNB139 plasmid was introduced in the *perRB* mutant
689 (M1474) by conjugation using the *E. coli* β2163 conjugating strain as previously described
690 [66]. *Leptospira* conjugants were selected on EMJH plates containing 50 µg/ml
691 spectinomycin and resistant colonies were then inoculated into liquid EMJH medium
692 supplemented with spectinomycin for further analysis. The restoration of *PerRB* expression in
693 the complemented *perRB* mutant was verified by RT-qPCR.

694 The double *perRAperRB* mutant *(ΔperRA, perRB::Km^R)* complementation required the
695 construction of a gentamycin resistant pMaORI complementation vector. A gentamycin
696 resistant cassette [67] was cloned into the pMaORI between the Not1 and Xba1 restriction
697 sites and the integrity of the gentamycin resistance cassette in the pMaORIgenta plasmid (S10
698 Table) was checked by DNA sequencing. Then, the *perRB* ORF (LIMLP_05620) together
699 with its native promoter region (248 bp upstream region) were amplified (using the F-ApaI-
700 PerR2genta and R-ApaI-PerR2genta primer set, S11 Table) from genomic DNA of *L.*
701 *interrogans* serovar Manilae strain L495 and cloned into the PCR-blunt II TOPO vector (Zero
702 Blunt TOPO PCR cloning kit, Invitrogen). The *perRB* locus was subsequently subcloned into
703 the pMaORIgenta plasmid at the ApaI restriction site. The obtained plasmid (pCZ3, S10
704 Table) or the empty pMaORIgenta plasmids were introduced in *perRAperRB* double

bioRxiv preprint doi: https://doi.org/10.1101/2020.11.06.371039; this version posted November 6, 2020. The copyright holder for this preprint (which was not certified by peer review) is the author/funder, who has granted bioRxiv a license to display the preprint in perpetuity. It is made available under aCC-BY 4.0 International license.

705 *Leptospira* mutant strain by conjugation using the *E. coli* β2163 conjugating strain as
706 previously described [66]. *Leptospira* conjugants were selected on EMJH plates containing 8
707 µg/ml gentamycin and resistant colonies were then inoculated into liquid EMJH medium
708 supplemented with gentamycin and spectinomycin for further analysis. The restoration of
709 *PerRB* expression in the trans-complemented double *perRAperRB* mutant was verified by RT-
710 qPCR (S4 Fig).
711
712 **Phylogenetic analyses**
713 The sequences homologous to the LIMLP_10155 (PerRA), LIMLP_05620 (PerRB),
714 LIMLP_18590 and LIMLP_04825 proteins were searched with BLASTP version 2.10.0
715 among the other *Leptospira* species (Fig 3 and S1 Table) or among the protein sequences of
716 11,070 representative genomes (Fig 2), as previously described [68]. In that case, only the
717 sequences with an e-value less than 1e-10 and a percentage of similarity greater than 60%
718 were retained. Sequences with percent identity equal to 100% were clustered by CD-HIT
719 version 4.8.1 and only one sequence was retained. The resulting 1671 sequences were
720 subsequently aligned by MAFFT version 7.471. A phylogenetic tree was finally built with IQ-
721 TREE version 2.1.1 under the best-fit model LG + R10. A second phylogenetic tree was made
722 with a subset of sequences to improve the resolution of the separation between PerRA and
723 PerRB. The same procedure was followed, except that the best-fit model used for
724 phylogenetic reconstruction is LG + R5. Both trees were visualized with FigTree version
725 1.4.4 (https://github.com/rambaut/figtree).
726
727 **RNA purification**
728 Virulent *L. interrogans* serovar Manilae strain L495 and *perRB* (M1474) mutant strains with
729 less than three *in vitro* passages were used in this study. Four independent biological

bioRxiv preprint doi: https://doi.org/10.1101/2020.11.06.371039; this version posted November 6, 2020. The copyright holder for this preprint (which was not certified by peer review) is the author/funder, who has granted bioRxiv a license to display the preprint in perpetuity. It is made available under aCC-BY 4.0 International license.

730 replicates of exponentially grown *L. interrogans* WT, *perRB* (M1474) and double
731 *perRAperRB* mutant strains were harvested and resuspended in 1 ml TRIzol (ThermoFisher
732 Scientific) and stored at -80°C. Nucleic Acids were extracted with chloroform and
733 precipitated with isopropanol as described earlier [69]. Contaminating genomic DNA was
734 removed by DNAse treatment using the RNAse-free Turbo DNA-free turbo kit
735 (ThermoFisher Scientific) as described by the manufacturer. The integrity of RNAs (RIN >
736 8.0) was verified by the Agilent Bioanalyzer RNA NanoChips (Agilent technologies,
737 Wilmington, DE).
738
739 **RNA Sequencing**
740 rRNA were depleted from 0.5 µg of total RNA using the Ribo-Zero rRNA Removal Kit
741 (Bacteria) from Illumina. Sequencing libraries were constructed using the TruSeq Stranded
742 mRNA Sample preparation kit (20020595) following the manufacturer's instructions
743 (Illumina). The directional libraries were controlled on Bioanalyzer DNA1000 Chips (Agilent
744 Technologies) and concentrations measured with the Qubit dsDNA HS Assay Kit
745 (ThermoFisher). Sequences of 65 bases were generated on the Illumina Hiseq 2500
746 sequencer.
747 Bioinformatics analyses were performed using the RNA-seq pipeline from Sequana [70].
748 Reads were cleaned of adapter sequences and low-quality sequences using cutadapt version
749 1.11 [71]. Only sequences at least 25 nt in length were considered for further analysis. Bowtie
750 version 1.2.2 [72], with default parameters, was used for alignment on the reference genome
751 (*L. interrogans* serovar Manilae strain UP-MMC-NIID LP, from MicroScope Platform).
752 Genes were counted using featureCounts version 1.4.6-p3 [73] from Subreads package
753 (parameters: -t gene -g locus_tag -s 1).

bioRxiv preprint doi: https://doi.org/10.1101/2020.11.06.371039; this version posted November 6, 2020. The copyright holder for this preprint (which was not certified by peer review) is the author/funder, who has granted bioRxiv a license to display the preprint in perpetuity. It is made available under aCC-BY 4.0 International license.

754 Count data were analyzed using R version 3.5.1 [74] and the Bioconductor package DESeq2
755 version 1.20.0 [75]. The normalization and dispersion estimation were performed with
756 DESeq2 using the default parameters and statistical tests for differential expression were
757 performed applying the independent filtering algorithm. Differential expressions were
758 expressed as logarithm to base 2 of fold change (Log_2FC). A generalized linear model
759 including the replicate effect as blocking factor was set in order to test for the differential
760 expression between *Leptospira* samples. Raw p-values were adjusted for multiple testing
761 according to the Benjamini and Hochberg (BH) procedure [76] and genes with an adjusted p-
762 value lower than 0.05 and a Log_2FC higher than 1 or lower than -1 were considered
763 differentially expressed. Heat maps and Volcano plots were generated using the Galaxy
764 platform (https://usegalaxy.eu/).
765
766 **Quantitative RT-PCR experiments**
767 cDNA synthesis was performed with the cDNA synthesis kit (Biorad) according to the
768 manufacturer's recommendation. Quantitative PCR was conducted in triplicate with the
769 SsoFast EvaGreen Supermix (Biorad) as previously described. LIMLP_06735 was used as a
770 reference gene.
771
772 **Non-coding RNA identification**
773 Sequencing data from the *L. interrogans* WT, *perRB* (M1474) and double *perRAperRB*
774 mutant strains were processed with Trimmomatic [77] to remove low-quality bases and
775 adapter contaminations. BWA mem (version 0.7.12) was used to discard the reads matching
776 *Leptospira* rRNA, tRNA or polyA sequences and to assign the resulting reads to *Leptospira*
777 replicons. Then Rockhopper [78] was used to re-align reads corresponding to separate
778 replicons and to assemble transcripts models. The output was filtered to retain all transcripts

bioRxiv preprint doi: https://doi.org/10.1101/2020.11.06.371039; this version posted November 6, 2020. The copyright holder for this preprint (which was not certified by peer review) is the author/funder, who has granted bioRxiv a license to display the preprint in perpetuity. It is made available under aCC-BY 4.0 International license.

779 longer than 50 nucleotides not overlapping within 10 nucleotides with NCBI annotated genes
780 on the same orientation, and showing a minimum Rockhopper raw count value of 50 in at
781 least two isolates. This high-quality set of new sRNA was subjected to differential expression
782 analysis with Rockhopper, adopting a Benjamini-Hochberg adjusted P-value threshold of
783 0.01. For each non-coding RNAs, putative function was identified by BLAST using the Rfam
784 database [79].
785
786 **Infection experiments**
787 WT and mutant *L. interrogans* strains were cultivated in EMJH medium until the exponential
788 phase and counted under a dark-field microscope using a Petroff-Hauser cell. 10^4 or 10^6
789 bacteria (in 0.5 ml) were injected intraperitoneally in groups of 4-8 male 4 weeks-old Syrian
790 Golden hamsters (RjHan:AURA, Janvier Labs). Animals were monitored daily and sacrificed
791 by carbon dioxide inhalation when endpoint criteria were met (sign of distress, morbidity).
792
793 **Ethics Statement**
794 The protocol for animal experimentation was reviewed by the Institut Pasteur (Paris, France),
795 the competent authority, for compliance with the French and European regulations on Animal
796 Welfare and with Public Health Service recommendations. This project has been reviewed
797 and approved (CETEA #2016-0019) by the Institut Pasteur ethic committee for animal
798 experimentation, agreed by the French Ministry of Agriculture.
799

800 ## Acknowledgement
801 The authors would like to thank Melissa Caimano and André Grassmann for fruitful
802 discussions.
803

bioRxiv preprint doi: https://doi.org/10.1101/2020.11.06.371039; this version posted November 6, 2020. The copyright holder for this preprint (which was not certified by peer review) is the author/funder, who has granted bioRxiv a license to display the preprint in perpetuity. It is made available under aCC-BY 4.0 International license.

Funding

Crispin Zavala-Alvarado was part of the Pasteur - Paris University (PPU) International PhD Program. This project has received funding from the European Union's Horizon 2020 research and innovation programme (https://ec.europa.eu/programmes/horizon2020/en) under the Marie Sklodowska-Curie grant agreement No 665807 (https://ec.europa.eu/research/mariecurieactions) and from Fondation Etchebès-Fondation France (S-CM 16008) (https://www.fondationdefrance.org/fr/fondation/fondation-etchebes). The funders had no role in study design, data collection and analysis, decision to publish, or preparation of the manuscript.

bioRxiv preprint doi: https://doi.org/10.1101/2020.11.06.371039; this version posted November 6, 2020. The copyright holder for this preprint (which was not certified by peer review) is the author/funder, who has granted bioRxiv a license to display the preprint in perpetuity. It is made available under aCC-BY 4.0 International license.

References

1. Haake DA, Levett PN. Leptospirosis in humans. Curr Top Microbiol Immunol. 2015;387:65-97.

2. Costa F, Hagan JE, Calcagno J, Kane M, Torgerson P, Martinez-Silveira MS, et al. Global Morbidity and Mortality of Leptospirosis: A Systematic Review. PLoS Negl Trop Dis. 2015;9(9):e0003898-e0003898.

3. Pijnacker R, Goris MGA, te Wierik MJM, Broens EM, van der Giessen JWB, de Rosa M, et al. Marked increase in leptospirosis infections in humans and dogs in the Netherlands, 2014. Eurosurveillance [Internet]. 2016;21(17). https://www.eurosurveillance.org/content/10.2807/1560-7917.ES.2016.21.17.30211

4. Ko AI, Goarant C, Picardeau M. Leptospira: the dawn of the molecular genetics era for an emerging zoonotic pathogen. Nat Rev Microbiol. 2009;7(10):736-47.

5. Picardeau M. Virulence of the zoonotic agent of leptospirosis: still terra incognita? Nat Rev Microbiol. 2017;15(5):297-307.

6. Imlay JA. Where in the world do bacteria experience oxidative stress? Environmental Microbiology. 2019;21(2):521-30.

7. Winterbourn CC, Kettle AJ. Redox Reactions and Microbial Killing in the Neutrophil Phagosome. Antioxidants & Redox Signaling. 2012;18(6):642-60.

8. Marangoni A, Accardo S, Aldini R, Guardigli M, Cavrini F, Sambri V, et al. Production of reactive oxygen species and expression of inducible nitric oxide synthase in rat isolated Kupffer cells stimulated by Leptospira interrogans and Borrelia burgdorferi. World J Gastroenterol. 2006;12(19):3077-81.

9. Araújo AM, Reis EAG, Athanazio DA, Ribeiro GS, Hagan JE, Araujo GC, et al. Oxidative stress markers correlate with renal dysfunction and thrombocytopenia in severe leptospirosis. Am J Trop Med Hyg. 2014;90(4):719-23.

10. Erdogan HM, Karapehlivan M, Citil M, Atakisi O, Uzlu E, Unver A. Serum sialic acid and oxidative stress parameters changes in cattle with leptospirosis. Veterinary Research Communications. 2008;32(4):333-9.

11. Eshghi A, Lourdault K, Murray GL, Bartpho T, Sermswan RW, Picardeau M, et al. Leptospira interrogans Catalase Is Required for Resistance to H2O2 and for Virulence. Blanke SR, éditeur. Infect Immun. 2012;80(11):3892.

12. Dubbs JM, Mongkolsuk S. Peroxide-sensing transcriptional regulators in bacteria. J Bacteriol. 2012;194(20):5495-503.

13. Choi H-J, Kim S-J, Mukhopadhyay P, Cho S, Woo J-R, Storz G, et al. Structural Basis of the Redox Switch in the OxyR Transcription Factor. Cell. 2001;105(1):103-13.

14. Zheng M, Åslund F, Storz G. Activation of the OxyR Transcription Factor by Reversible Disulfide Bond Formation. Science. 1998;279(5357):1718.

15. Herbig AF, Helmann JD. Roles of metal ions and hydrogen peroxide in modulating the interaction of the Bacillus subtilis PerR peroxide regulon repressor with operator DNA. Mol Microbiol. 2001;41(4):849-59.

16. Jacquamet L, Traoré D a. K, Ferrer J-L, Proux O, Testemale D, Hazemann J-L, et al. Structural characterization of the active form of PerR: insights into the metal-induced

bioRxiv preprint doi: https://doi.org/10.1101/2020.11.06.371039; this version posted November 6, 2020. The copyright holder for this preprint (which was not certified by peer review) is the author/funder, who has granted bioRxiv a license to display the preprint in perpetuity. It is made available under aCC-BY 4.0 International license.

activation of PerR and Fur proteins for DNA binding. Mol Microbiol. 2009;73(1):20-31.

17. Traoré DAK, El Ghazouani A, Ilango S, Dupuy J, Jacquamet L, Ferrer J-L, et al. Crystal structure of the apo-PerR-Zn protein from Bacillus subtilis. Mol Microbiol. 2006;61(5):1211-9.

18. Lee J-W, Helmann JD. The PerR transcription factor senses H2O2 by metal-catalysed histidine oxidation. Nature. 2006;440(7082):363-7.

19. Traoré DAK, El Ghazouani A, Jacquamet L, Borel F, Ferrer J-L, Lascoux D, et al. Structural and functional characterization of 2-oxo-histidine in oxidized PerR protein. Nat Chem Biol. 2009;5(1):53-9.

20. Nunoshiba T, Hidalgo E, Amábile Cuevas CF, Demple B. Two-stage control of an oxidative stress regulon: the Escherichia coli SoxR protein triggers redox-inducible expression of the soxS regulatory gene. J Bacteriol. 1992;174(19):6054-60.

21. Wu J, Weiss B. Two-stage induction of the soxRS (superoxide response) regulon of Escherichia coli. J Bacteriol. 1992;174(12):3915-20.

22. Gu M, Imlay JA. The SoxRS response of Escherichia coli is directly activated by redox-cycling drugs rather than by superoxide. Mol Microbiol. 2011;79(5):1136-50.

23. Price CW, Fawcett P, Cérémonie H, Su N, Murphy CK, Youngman P. Genome-wide analysis of the general stress response in Bacillus subtilis. Mol Microbiol. 2001;41(4):757-74.

24. Lo M, Murray GL, Khoo CA, Haake DA, Zuerner RL, Adler B. Transcriptional response of Leptospira interrogans to iron limitation and characterization of a PerR homolog. Infect Immun. 2010;78(11):4850-9.

25. Austin FE, Barbieri JT, Corin RE, Grigas KE, Cox CD. Distribution of superoxide dismutase, catalase, and peroxidase activities among Treponema pallidum and other spirochetes. Infect Immun. 1981;33(2):372-9.

26. Fouts DE, Matthias MA, Adhikarla H, Adler B, Amorim-Santos L, Berg DE, et al. What Makes a Bacterial Species Pathogenic?: Comparative Genomic Analysis of the Genus Leptospira. PLOS Neglected Tropical Diseases. 2016;10(2):e0004403.

27. Zavala-Alvarado C, Sismeiro O, Legendre R, Varet H, Bussotti G, Bayram J, et al. The transcriptional response of pathogenic Leptospira to peroxide reveals new defenses against infection-related oxidative stress. PLOS Pathogens. 2020;16(10):e1008904.

28. Caux-Thang C, Parent A, Sethu R, Maïga A, Blondin G, Latour J-M, et al. Single asparagine to arginine mutation allows PerR to switch from PerR box to fur box. ACS Chem Biol. 2015;10(3):682-6.

29. Parent A, Caux-Thang C, Signor L, Clémancey M, Sethu R, Blondin G, et al. Single glutamate to aspartate mutation makes ferric uptake regulator (Fur) as sensitive to H2O2 as peroxide resistance regulator (PerR). Angew Chem Int Ed Engl. 2013;52(39):10339-43.

30. Kebouchi M, Saul F, Taher R, Landier A, Beaudeau B, Dubrac S, et al. Structure and function of the Leptospira interrogans peroxide stress regulator (PerR), an atypical PerR devoid of a structural metal-binding site. J Biol Chem. 2018;293(2):497-509.

31. Satou K, Shimoji M, Tamotsu H, Juan A, Ashimine N, Shinzato M, et al. Complete Genome Sequences of Low-Passage Virulent and High-Passage Avirulent Variants of Pathogenic Leptospira interrogans Serovar Manilae Strain UP-MMC-NIID, Originally Isolated from a Patient with Severe Leptospirosis, Determined Using PacBio Single-Molecule

bioRxiv preprint doi: https://doi.org/10.1101/2020.11.06.371039; this version posted November 6, 2020. The copyright holder for this preprint (which was not certified by peer review) is the author/funder, who has granted bioRxiv a license to display the preprint in perpetuity. It is made available under aCC-BY 4.0 International license.

898 Real-Time Technology. Genome Announc. 2015;3(4):e00882-15.

899 32. Domingos RF, Vieira ML, Romero EC, Gonçales AP, de Morais ZM, Vasconcellos
900 SA, et al. "Features of two proteins of Leptospira interrogans with potential role in host-
901 pathogen interactions". BMC Microbiology. 2012;12(1):50.

902 33. Thibeaux R, Soupé-Gilbert M-E, Kainiu M, Girault D, Bierque E, Fernandes J, et al.
903 The zoonotic pathogen Leptospira interrogans mitigates environmental stress through cyclic-
904 di-GMP-controlled biofilm production. npj Biofilms and Microbiomes. 2020;6(1):24.

905 34. Xiao G, Kong L, Che R, Yi Y, Zhang Q, Yan J, et al. Identification and
906 Characterization of c-di-GMP Metabolic Enzymes of Leptospira interrogans and c-di-GMP
907 Fluctuations After Thermal Shift and Infection. Frontiers in Microbiology. 2018;9:764.

908 35. Narayanavari SA, Lourdault K, Sritharan M, Haake DA, Matsunaga J. Role of sph2
909 Gene Regulation in Hemolytic and Sphingomyelinase Activities Produced by Leptospira
910 interrogans. PLOS Neglected Tropical Diseases. 2015;9(8):e0003952.

911 36. Caimano MJ, Sivasankaran SK, Allard A, Hurley D, Hokamp K, Grassmann AA, et
912 al. A Model System for Studying the Transcriptomic and Physiological Changes Associated
913 with Mammalian Host-Adaptation by Leptospira interrogans Serovar Copenhageni. PLOS
914 Pathogens. 2014;10(3):e1004004.

915 37. Bourhy P, Salaün L, Lajus A, Médigue C, Boursaux-Eude C, Picardeau M. A
916 Genomic Island of the Pathogen Leptospira interrogans Serovar Lai Can Excise from Its
917 Chromosome. Infect Immun. 2007;75(2):677.

918 38. He P, Sheng Y-Y, Shi Y-Z, Jiang X-G, Qin J-H, Zhang Z-M, et al. Genetic diversity
919 among major endemic strains of Leptospira interrogans in China. BMC Genomics.
920 2007;8:204-204.

921 39. Overton TW, Justino MC, Li Y, Baptista JM, Melo AMP, Cole JA, et al. Widespread
922 Distribution in Pathogenic Bacteria of Di-Iron Proteins That Repair Oxidative and Nitrosative
923 Damage to Iron-Sulfur Centers. J Bacteriol. 2008;190(6):2004.

924 40. Nambi S, Long JE, Mishra BB, Baker R, Murphy KC, Olive AJ, et al. The Oxidative
925 Stress Network of Mycobacterium tuberculosis Reveals Coordination between Radical
926 Detoxification Systems. Cell Host & Microbe. 2015;17(6):829-37.

927 41. Krajewska J, Modrak-Wójcik A, Arent ZJ, Więckowski D, Zolkiewski M, Bzowska
928 A, et al. Characterization of the molecular chaperone ClpB from the pathogenic spirochaete
929 Leptospira interrogans. PLOS ONE. 2017;12(7):e0181118.

930 42. Lourdault K, Cerqueira GM, Wunder EA, Picardeau M. Inactivation of clpB in the
931 pathogen Leptospira interrogans reduces virulence and resistance to stress conditions. Infect
932 Immun. 2011;79(9):3711-7.

933 43. Choy HA, Kelley MM, Chen TL, Møller AK, Matsunaga J, Haake DA. Physiological
934 osmotic induction of Leptospira interrogans adhesion: LigA and LigB bind extracellular
935 matrix proteins and fibrinogen. Infect Immun. 2007;75(5):2441-50.

936 44. Castiblanco-Valencia MM, Fraga TR, Silva LB da, Monaris D, Abreu PAE, Strobel S,
937 et al. Leptospiral Immunoglobulin-like Proteins Interact With Human Complement
938 Regulators Factor H, FHL-1, FHR-1, and C4BP. The Journal of Infectious Diseases.
939 2012;205(6):995-1004.

940 45. Pappas CJ, Picardeau M. Control of Gene Expression in Leptospira spp. by
941 Transcription Activator-Like Effectors Demonstrates a Potential Role for LigA and LigB in

bioRxiv preprint doi: https://doi.org/10.1101/2020.11.06.371039; this version posted November 6, 2020. The copyright holder for this preprint (which was not certified by peer review) is the author/funder, who has granted bioRxiv a license to display the preprint in perpetuity. It is made available under aCC-BY 4.0 International license.

942 Leptospira interrogans Virulence. Appl Environ Microbiol. 2015;81(22):7888-92.

943 46. Adhikarla H, Wunder EA Jr, Mechaly AE, Mehta S, Wang Z, Santos L, et al. Lvr, a
944 Signaling System That Controls Global Gene Regulation and Virulence in Pathogenic
945 Leptospira. Front Cell Infect Microbiol. 2018;8:45-45.

946 47. Yuan Y, Crane DD, Simpson RM, Zhu Y, Hickey MJ, Sherman DR, et al. The 16-kDa
947 α-crystallin (Acr) protein of Mycobacterium tuberculosis is required for growth
948 in macrophages. Proc Natl Acad Sci USA. 1998;95(16):9578.

949 48. Murray GL, Srikram A, Henry R, Puapairoj A, Sermswan RW, Adler B. Leptospira
950 interrogans requires heme oxygenase for disease pathogenesis. Microbes and Infection.
951 2009;11(2):311-4.

952 49. Hayashi K, Ohsawa T, Kobayashi K, Ogasawara N, Ogura M. The H2O2 Stress-
953 Responsive Regulator PerR Positively Regulates srfA Expression in Bacillus subtilis. Journal
954 of Bacteriology. 2005;187(19):6659–6667.

955 50. Palyada K, Sun Y-Q, Flint A, Butcher J, Naikare H, Stintzi A. Characterization of the
956 oxidative stress stimulon and PerR regulon of Campylobacter jejuni. BMC Genomics.
957 2009;10(1):481.

958 51. Mostertz J, Scharf C, Hecker M, Homuth G. Transcriptome and proteome analysis of
959 Bacillus subtilis gene expression in response to superoxide and peroxide stress. Vol. 150,
960 Microbiology. 2004. p. 497-512.

961 52. Zhou A, He Z, Redding-Johanson AM, Mukhopadhyay A, Hemme CL, Joachimiak
962 MP, et al. Hydrogen peroxide-induced oxidative stress responses in Desulfovibrio vulgaris
963 Hildenborough. Environmental Microbiology. 2010;12(10):2645-57.

964 53. Fuangthong M, Herbig AF, Bsat N, Helmann JD. Regulation of the Bacillus subtilis
965 fur and perR Genes by PerR: Not All Members of the PerR Regulon Are Peroxide Inducible.
966 Journal of Bacteriology. 2002;184(12):3276–3286.

967 54. Horsburgh MJ, Ingham E, Foster SJ. In Staphylococcus aureus, Fur Is an Interactive
968 Regulator with PerR, Contributes to Virulence, and Is Necessary for Oxidative Stress
969 Resistance through Positive Regulation of Catalase and Iron Homeostasis. Journal of
970 Bacteriology. 2001;183(2):468–475.

971 55. Kim J-H, Ji C-J, Ju S-Y, Yang Y-M, Ryu S-H, Kwon Y, et al. Bacillus licheniformis
972 Contains Two More PerR-Like Proteins in Addition to PerR, Fur, and Zur Orthologues.
973 PLOS ONE. 2016;11(5):e0155539.

974 56. Lee H-N, Ji C-J, Lee H-H, Park J, Seo Y-S, Lee J-W, et al. Roles of three FurA
975 paralogs in the regulation of genes pertaining to peroxide defense in Mycobacterium
976 smegmatis mc2155. Molecular Microbiology. 2018;108(6):661-82.

977 57. Grassmann AA, Zavala-Alvarado C, Bettin E, Picardeau M, Benaroudj N, Caimano
978 MJ. The Fur-like regulators PerRA and PerRB control a complex signaling network required
979 for mammalian host-adpatation and virulence of Leptospira interrogans. submitted. 2020;

980 58. Brenot A, King KY, Caparon MG. The PerR regulon in peroxide resistance and
981 virulence of Streptococcus pyogenes. Molecular Microbiology. 2005;55(1):221-34.

982 59. Rea RB, Gahan CGM, Hill C. Disruption of putative regulatory loci in Listeria
983 monocytogenes demonstrates a significant role for Fur and PerR in virulence. Infect Immun.
984 2004;72(2):717-27.

985 60. Ricci S, Janulczyk R, Björck L. The Regulator PerR Is Involved in Oxidative Stress

bioRxiv preprint doi: https://doi.org/10.1101/2020.11.06.371039; this version posted November 6, 2020. The copyright holder for this preprint (which was not certified by peer review) is the author/funder, who has granted bioRxiv a license to display the preprint in perpetuity. It is made available under aCC-BY 4.0 International license.

Response and Iron Homeostasis and Is Necessary for Full Virulence of Streptococcus pyogenes. Infect Immun. 2002;70(9):4968.

61. Wu H-J, Seib KL, Srikhanta YN, Kidd SP, Edwards JL, Maguire TL, et al. PerR controls Mn-dependent resistance to oxidative stress in Neisseria gonorrhoeae. Molecular Microbiology. 2006;60(2):401‑16.

62. Stewart GR, Newton SM, Wilkinson KA, Humphreys IR, Murphy HN, Robertson BD, et al. The stress-responsive chaperone α-crystallin 2 is required for pathogenesis of Mycobacterium tuberculosis. Molecular Microbiology. 2005;55(4):1127‑37.

63. Ellinghausen HC, Mccullough WG. Nutrition of Leptospira pomona and growth of 13 other serotypes: a serum-free medium employing oleic albumin complex. Am J Vet Res. 1965;26:39‑44.

64. Picardeau M, Brenot A, Saint Girons I. First evidence for gene replacement in Leptospira spp. Inactivation of L. biflexa flaB results in non-motile mutants deficient in endoflagella. Molecular Microbiology. 2001;40(1):189‑99.

65. Pappas CJ, Benaroudj N, Picardeau M. A Replicative Plasmid Vector Allows Efficient Complementation of Pathogenic Leptospira Strains. Parales RE, éditeur. Appl Environ Microbiol. 2015;81(9):3176.

66. Picardeau M. Conjugative transfer between Escherichia coli and Leptospira spp. as a new genetic tool. Appl Environ Microbiol. 2008;74(1):319‑22.

67. Poggi D, Oliveira de Giuseppe P, Picardeau M. Antibiotic resistance markers for genetic manipulations of Leptospira spp. Appl Environ Microbiol. 2010;76(14):4882‑5.

68. Vincent AT, Schiettekatte O, Goarant C, Neela VK, Bernet E, Thibeaux R, et al. Revisiting the taxonomy and evolution of pathogenicity of the genus Leptospira through the prism of genomics. PLoS Negl Trop Dis. 2019;13(5):e0007270‑e0007270.

69. Zavala-Alvarado C, Benaroudj N. The Single-Step Method of RNA Purification Applied to Leptospira. Methods Mol Biol. 2020;2134:41‑51.

70. Cokelaer, T, Desvillechabrol, D, Legendre, R, Cardon, M. ‘Sequana’: a Set of Snakemake NGS pipelines. The Journal of Open Source Software. 2(16).

71. Martin M. Cutadapt removes adapter sequences from high-throughput sequencing reads. EMBnet.journal; Vol 17, No 1: Next Generation Sequencing Data AnalysisDO - 1014806/ej171200 [Internet]. 2011; http://journal.embnet.org/index.php/embnetjournal/article/view/200

72. Langmead B, Trapnell C, Pop M, Salzberg SL. Ultrafast and memory-efficient alignment of short DNA sequences to the human genome. Genome Biology. 2009;10(3):R25.

73. Liao Y, Smyth GK, Shi W. featureCounts: an efficient general purpose program for assigning sequence reads to genomic features. Bioinformatics. 2013;30(7):923‑30.

74. R core Team. R, a language and environment for statistcial computing [Internet]. 2016. https://www.gbif.org/en/tool/81287/r-a-language-and-environment-for-statistical-computing

75. Love MI, Huber W, Anders S. Moderated estimation of fold change and dispersion for RNA-seq data with DESeq2. Genome Biology. 2014;15(12):550.

76. Benjamini Y, Hochberg Y. Controlling the False Discovery Rate: A Practical and Powerful Approach to Multiple Testing. Journal of the Royal Statistical Society Series B

bioRxiv preprint doi: https://doi.org/10.1101/2020.11.06.371039; this version posted November 6, 2020. The copyright holder for this preprint (which was not certified by peer review) is the author/funder, who has granted bioRxiv a license to display the preprint in perpetuity. It is made available under aCC-BY 4.0 International license.

(Methodological). 1995;57(1):289-300.

77. Bolger AM, Lohse M, Usadel B. Trimmomatic: a flexible trimmer for Illumina sequence data. Bioinformatics. 2014;30(15):2114-20.

78. McClure R, Balasubramanian D, Sun Y, Bobrovskyy M, Sumby P, Genco CA, et al. Computational analysis of bacterial RNA-Seq data. Nucleic Acids Res. 2013;41(14):e140-e140.

79. Kalvari I, Argasinska J, Quinones-Olvera N, Nawrocki EP, Rivas E, Eddy SR, et al. Rfam 13.0: shifting to a genome-centric resource for non-coding RNA families. Nucleic Acids Research. 2017;46(D1):D335-42.

80. Madeira F, Park Y mi, Lee J, Buso N, Gur T, Madhusoodanan N, et al. The EMBL-EBI search and sequence analysis tools APIs in 2019. Nucleic Acids Research. 2019;47(W1):W636-41.

81. Kelley LA, Mezulis S, Yates CM, Wass MN, Sternberg MJE. The Phyre2 web portal for protein modeling, prediction and analysis. Nature Protocols. 2015;10(6):845-58.

bioRxiv preprint doi: https://doi.org/10.1101/2020.11.06.371039; this version posted November 6, 2020. The copyright holder for this preprint (which was not certified by peer review) is the author/funder, who has granted bioRxiv a license to display the preprint in perpetuity. It is made available under aCC-BY 4.0 International license.

Supporting information

S1 Fig. Phylogenetic analysis of the four Fur-like regulators of *L. interrogans*.

Extended phylogenetic tree showing the separation between PerRA (red) and PerRB (blue).

S2 Fig. Growth of the *L. interrogans perRA* and *perRB* mutants in the presence of H_2O_2.

L. interrogans WT (black circles), *perRA* (cyan up-pointing triangles) and *perRB* (green down-pointing triangles) mutant strains were cultivated in EMJH medium at 30°C in the absence (A) or presence of 2 mM H_2O_2 (B). *Leptospira* growth was assessed by absorbance at 420 nm. Data are means and standard errors of three independent biological experiments.

S3 Fig. Analysis of the *L. interrogans* PerRB regulon.

(A) Venn diagram showing the overlap of differentially-expressed ORFs (with an adjusted p-value < 0.05) in the *perRA* and *perRB* mutants. Differentially-expressed genes in the *perRB* mutant (as determined in this study) (in green) were compared with those in the *perRA* mutant as determined previously [27] (in cyan). The down- and up-regulated ORFs in both mutants were indicated in blue and red, respectively. (B) Comparison of differentially-expressed ORFs (with an adjusted p-value < 0.05) in the *perRB* mutant and upon *L. interrogans* exposure to H_2O_2. Log_2FC of differentially-expressed ORFs upon *L. interrogans* exposure to 1 mM H_2O_2 (as determined previously [27] was plotted against the Log_2FC of differentially-expressed ORFs upon *perRB* inactivation. Down- and up-regulated ORFs in the *perRB* mutant were represented by blue and red symbols, respectively, and the name of selected ORFs was indicated. The dashed lines indicate a Log_2FC value of zero. Please note that only differentially-expressed ORFs in both conditions were considered.

bioRxiv preprint doi: https://doi.org/10.1101/2020.11.06.371039; this version posted November 6, 2020. The copyright holder for this preprint (which was not certified by peer review) is the author/funder, who has granted bioRxiv a license to display the preprint in perpetuity. It is made available under aCC-BY 4.0 International license.

S4 Fig. Characterization and complementation of the double *perRAperRB* mutant strain. (A) Schematic representation of the double *perRAperRB* mutant construction. *PerRA* (LIMLP_10155) was inactivated by allelic exchange in the transposon *perRB* mutant. The kanamycin (Km) and spectinomycin (Spc) resistance cassettes inactivating *perRB* and *perRA*, respectively, are indicated. (B) Production of PerRA in the WT, in the single *perRA* and *perRB* mutants and in the double *perRAperRB* mutant strains. *L. interrogans* strains were cultivated in EMJH medium at 30°C until the logarithmic phase and lyzed by sonication. 10 µg of total lyzates were resolved on a 15% SDS-PAGE and transferred on nitrocellulose membrane. PerRA was detected by immunoblot using a 1/2000 antibody dilution as described previously [30]. (C) *PerRB* expression in the WT, in the double *perRAperRB* mutant and in the trans-complemented *perRAperRB* mutant with the *perRB* ORF. RNAs were extracted from exponentially-grown *L. interrogans* strains and *perRB* expression was assessed by RT-qPCR in triplicate using *flaB* gene (LIMLP_09410) as reference gene. *PerRB* expression in the *perRAperRB* and trans-complemented mutant strains were normalized against that in the WT strain. (D) Growth of stationary phase-adapted WT, *perRAperRB* and trans-complemented *perRAperRB* mutant strains. *L. interrogans* WT (black circles), *perRAperRB* mutant (pink squares) and *perRAperRB* mutant trans-complemented with the *perRB* ORF (blue triangles) were cultivated in EMJH medium at 30°C until late stationary phase (7 days after the entry in the stationary phase) and used to inoculate EMJH medium. Bacteria were then cultivated at 30°C and growth was assessed by absorbance at 420 nm. Data are means and standard errors of three independent biological experiments.

S5 Fig. RT-qPCR experiments in the double *perRAperRB* mutant.

RNAs were extracted from exponentially-grown *L. interrogans* strains WT or double

bioRxiv preprint doi: https://doi.org/10.1101/2020.11.06.371039; this version posted November 6, 2020. The copyright holder for this preprint (which was not certified by peer review) is the author/funder, who has granted bioRxiv a license to display the preprint in perpetuity. It is made available under aCC-BY 4.0 International license.

perRAperRB mutant (*m*). Expression of the indicated genes was measured by RT-qPCR using the LIMLP_06735 as reference gene. Gene expression in the *perRAperRB* mutant was normalized against that in the WT strain. Fold change values are indicated in blue. Statistical significance was determined by a Two-way Anova test in comparison with the WT samples. ****, p-value<0.0001; **, p-value<0.005.

S1 Table. Distribution of the four Fur-like regulators of *Leptospira interrogans* in the genus *Leptospira*.

S2 Table. Complete set of ORF expression in *Leptospira interrogans* WT and M1474 *perRB* mutant.

S3 Table. Complete set of ORF expression in *Leptospira interrogans* WT and double *perRAperRB* mutant.

S4 Table. Selected down-regulated genes in the *perRAperRB* double mutant.

S5 Table. Selected up-regulated genes in the *perRAperRB* double mutant.

S6 Table. Complete set of differentially-expressed predicted non coding RNAs in the *perRB* (M1474) and in the double *perRAperRB* mutant strains of *Leptospira interrogans*.

S7 Table. Selected differentially-expressed non-coding RNAs in the *perRB* mutant

S8 Table. Selected differentially-expressed non-coding RNAs in the *perRAperRB* mutant.

bioRxiv preprint doi: https://doi.org/10.1101/2020.11.06.371039; this version posted November 6, 2020. The copyright holder for this preprint (which was not certified by peer review) is the author/funder, who has granted bioRxiv a license to display the preprint in perpetuity. It is made available under aCC-BY 4.0 International license.

S9 Table. Strains used in this study

S10 Table. Plasmids used in this study

S11 Table. Primers used in this study

bioRxiv preprint doi: https://doi.org/10.1101/2020.11.06.371039; this version posted November 6, 2020. The copyright holder for this preprint (which was not certified by peer review) is the author/funder, who has granted bioRxiv a license to display the preprint in perpetuity. It is made available under aCC-BY 4.0 International license.

Figure legends

Fig 1. Analysis of the four Fur-like regulators of *L. interrogans*.

(A) Schematic representation of the domain organization of a typical Fur-like regulator. The N-terminal DNA binding domain and the C-terminal dimerization domain are represented in grey and golden, respectively. The α-helix and β-strand secondary structures are indicated below in green and blue, respectively. The His, Asp and Glu residues involved in regulatory metal coordination are designated in green. The Arg/Asn residue involved in DNA binding specificity is marked in red. The Arg/Asn (involved in DNA binding specificity) and Asp/Glu residues (involved in H_2O_2 sensitivity) that allow distinguishing a Fur from a PerR are further emphasized with a grey arrow head. The two cysteinate motifs in the C-terminal domain involved in structural metal coordination are represented by the double blue lines in the C-terminal dimerization domain. (B) Comparison of the four Fur-like regulators of *L. interrogans* (LIMLP_10155, LIMLP_05620, LIMLP_04825, LIMLP_18590) with *B. subtilis* Fur and PerR. Primary sequence alignment was obtained by Clustal Omega (https://www.ebi.ac.uk/Tools/msa/clustalo/; [80]). The H4 DNA binding helix is underlined and the Arg/Asn residue involved in DNA binding specificity is designated in red. The residues of the regulatory metal coordination, including the Asp/Glu residue involved in H_2O_2 sensitivity, are marked in green and indicated with an asterisk. The Arg/Asn and Asp/Glu residues that allow distinguishing a Fur from a PerR are further emphasized with a grey arrow head. The cysteine residues of the structural metal coordination are marked in cyan. (C) Cartoon representation of the crystal structure of LIMLP_10155 (5NL9) and of the modeled structure of LIMLP_05620, LIMLP_04825 and LIMLP_18590. The modeled structures were obtained by searching homologies between LIMLP_05620, LIMLP_04825 and

bioRxiv preprint doi: https://doi.org/10.1101/2020.11.06.371039; this version posted November 6, 2020. The copyright holder for this preprint (which was not certified by peer review) is the author/funder, who has granted bioRxiv a license to display the preprint in perpetuity. It is made available under aCC-BY 4.0 International license.

1151 LIMLP_18590 and protein with known crystal structure using PHYRE2
1152 (http://www.sbg.bio.ic.ac.uk/~phyre2/html/page.cgi?id=index; [81]). Secondary structures are
1153 numbered as in (A).
1154
1155 **Fig 2.** (A) Phylogenetic tree with a cartoon representation showing the distribution of the
1156 1671 sequences putatively homologous to the LIMLP_10155 (PerRA, cyan triangle),
1157 LIMLP_05620 (PerRB, green triangle), LIMLP_18590 (yellow triangle) and LIMLP_04825
1158 (red triangle) proteins. The gray triangles represent groups which are not monophyletic with
1159 the *Leptospira* sequences and which may therefore originate from other types of PerR or have
1160 had a species-specific evolution. (B) Phylogenetic tree showing the separation between
1161 PerRA (cyan) and PerRB (green).
1162
1163 **Fig 3. Distribution of the four Fur-like regulators of *L. interrogans* in the genus**
1164 ***Leptospira*.**
1165 Circular phylogenetic tree with inner circles indicating the homology between each Fur-like
1166 regulator of *L. interrogans* with the closest homolog among representative genomes of
1167 *Leptospira* species. The branches are colored according to their classification into the four
1168 main subclades with P1 (highly pathogenic) in red, P2 (intermediates) in magenta, S1
1169 (saprophytes) in yellow and S2 (new clade saprophytes) in blue [68]. The inner circles are,
1170 from the inside to the outside, LIMLP_10155, LIMLP_05620, LIMLP_04825 and
1171 LIMLP_18590. The green color gradient indicates the degree of homology (See S1 Table),
1172 grey and black indicate the presence of a false positive and the absence of orthologs,
1173 respectively.
1174
1175 **Fig 4. Increased *PerRA* and *perRB* expression upon exposure to hydrogen peroxide.**

bioRxiv preprint doi: https://doi.org/10.1101/2020.11.06.371039; this version posted November 6, 2020. The copyright holder for this preprint (which was not certified by peer review) is the author/funder, who has granted bioRxiv a license to display the preprint in perpetuity. It is made available under aCC-BY 4.0 International license.

Exponentially growing *L. interrogans* were incubated in the absence or presence of 10 µM (for 30 min.) or 1 mM H_2O_2 (for 60 min.) and *perRA* (cyan circles) and *perRB* (green squares) expression was measured by RT-qPCR as described in Material and Methods section. Gene expression was normalized by that in untreated samples. Data are the means and standard errors of three independent biological replicates. P-values obtained by a Two-way Anova test indicates the statistical significance in comparison with untreated samples.

Fig 5. Effect of *perRB* inactivation on *Leptospira* growth in the presence of superoxide-generating paraquat.

L. interrogans WT containing the empty pMaORI vector (black circles), the *perRB* mutant containing the empty pMaORI vector (green triangles) or the *perRB* mutant containing the pMaORI vector expressing LIMLP_05620 (red squares) were cultivated in EMJH medium in the absence (A) or in the presence of 2 µM Paraquat (B). Growth was assessed by measure of absorbance at 420 nm. Data are means and standard errors of three independent biological replicates.

Fig 6. Effect of concomitant inactivation of *perRA* and *perRB* on *Leptospira* growth in the presence of ROS and virulence.

L. interrogans WT (black circles), the single *perRA* mutant (cyan up-pointing triangles), the single *perRB* mutants (green down-pointing triangles) or the double *perRAperRB* mutant (pink squares) were cultivated in EMJH medium in the absence (A), or in the presence of 2 mM H_2O_2 (B) or of 2 µM paraquat (C). Complementation of the double *perRAperRB* mutant with *perRB* ORF (presented in (D)) was performed by cultivating *L. interrogans* WT containing the empty pMaORIgenta vector (black circles), the double *perRAperRB* mutant containing the empty pMaORIgenta vector (pink squares) or the double *perRAperRB* mutant

bioRxiv preprint doi: https://doi.org/10.1101/2020.11.06.371039; this version posted November 6, 2020. The copyright holder for this preprint (which was not certified by peer review) is the author/funder, who has granted bioRxiv a license to display the preprint in perpetuity. It is made available under aCC-BY 4.0 International license.

containing the pMaORIgenta vector expressing LIMLP_05620 (blue triangles) in the presence of 2 µM paraquat. Growth was assessed by measure of absorbance at 420 nm and the data are means and standard errors of three independent biological replicates. (E) Virulence was assessed by infecting hamsters (n=4) by peritoneal route with 10^4 of WT (black circles), single *perRA* or *perRB* mutants (cyan and green triangles, respectively), or the double *perRAperRB* mutant (pink squares) as described in Material and Methods section. (F) Complementation of the double *perRAperRB* mutant with *perRB* was performed by infecting hamsters (n=8) by peritoneal route with 10^6 of WT containing the empty pMaORIgenta vector (black circles), of the double *perRAperRB* mutant containing the empty pMaORIgenta vector (pink squares) or the double *perRAperRB* mutant containing the pMaORIgenta vector expressing LIMLP_05620 (blue triangles).

Fig 7. Differential gene expression in the *perRAperRB* mutant.

(A) Venn diagram showing the overlap of differentially-expressed ORFs (with an adjusted p-value < 0.05) in the double *perRAperRB* mutant (in pink) with those of the *perRA* mutant (as determined by Zavala-Alvarado *et al.* [27]) (in cyan) and of the *perRB* mutant (as determined in this study) (in green). (B)-(D) Volcano scatter representation of differentially-expressed genes in the *perRAperRB* mutant (B), in the single *perRA* mutant (as determined by Zavala-Alvarado *et al.* [27]) (C), and in the single *perRB* mutant (as determined in this study) (D). Red and blue dots indicate significantly up- and down-regulated genes, respectively, with a Log_2FC cutoff of ±1 (dashed vertical lines) and p-value<0.05. Selected genes are labelled.

Fig 8. Comparison of differential gene expression in the double *perRAperRB* mutant with that in the single *perRA* and *perRB* mutants.

Expression of selected genes of the TonB-dependent transport cluster (A), involved in

bioRxiv preprint doi: https://doi.org/10.1101/2020.11.06.371039; this version posted November 6, 2020. The copyright holder for this preprint (which was not certified by peer review) is the author/funder, who has granted bioRxiv a license to display the preprint in perpetuity. It is made available under aCC-BY 4.0 International license.

oxidative stress and redox homeostasis (B), in regulation and signaling (C), and in virulence (D) determined by RNASeq in the double *perRAperRB* mutant was compared to that in the single *perRA* mutant determined by Zavala-Alvarado *et al.* [27] and single *perRB* mutant (as determined in this study). Differential expression in each mutant strain was normalized with that in the WT strain. Gene names are indicated on the right. The Heat Map color from blue to red indicates low to high Log_2FC.

Fig 9. Complementation of the *perRAperRB* mutant with *perRB* restores expression of virulence associated genes.

The WT containing the empty pMaORIgenta vector (black circles), the *perRAperRB* mutant containing the empty pMaORIgenta vector (pink circles) and the complemented *perRAperRB* mutant (blue circles) strains were cultivated in EMJH medium until the exponential phase. Cells were harvested and RNAs were purified, and the expression of *lvrA*, *lvrB*, *ligA*, *ligB*, *clpB*, *hsp20* and *hsp15* was measured by RT-qPCR. Gene expression was normalized by that in the WT strains. Data are the means and standard errors of three independent biological replicates. P-values obtained by a Two-way Anova test indicates the statistical significance in comparison with WT samples.

Fig 10. Non-coding RNAs expression in the double *perRAperRB* mutant.

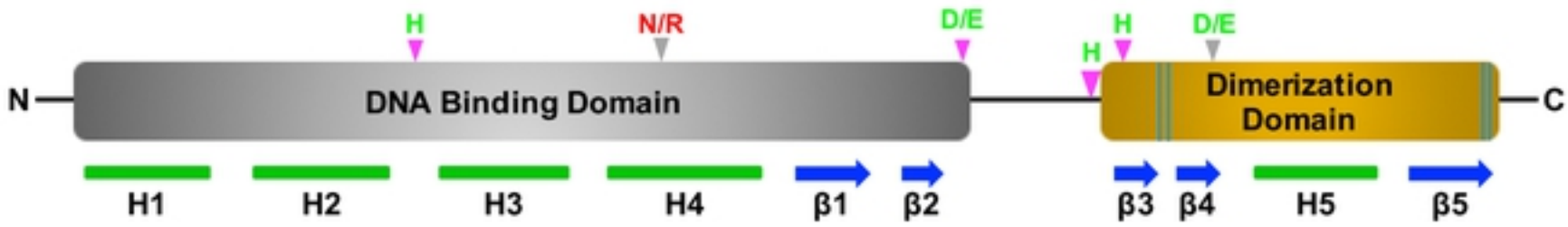
Differential expression of selected ncRNAs (LepncRNA38, 49, 105, and 130) in the *perRAperRB* mutant (determined in this study) ([a]) was compared to those in the single *perRA* mutant, as determined by Zavala-Alvarado *et al.* [27] ([b]), in the single *perRB* mutant (determined by this study) ([a]), and upon exposure to 1 mM H_2O_2 for 1h00 as determined by Zavala-Alvarado *et al.* [27] ([b]). The location of the ncRNAs LepncRNA38, 49, 105, and 130 were represented schematically with the adjacent or overlapping ORFs. The values indicate

bioRxiv preprint doi: https://doi.org/10.1101/2020.11.06.371039; this version posted November 6, 2020. The copyright holder for this preprint (which was not certified by peer review) is the author/funder, who has granted bioRxiv a license to display the preprint in perpetuity. It is made available under aCC-BY 4.0 International license.

1251 the Log_2FC of ncRNAs expression normalized with that in WT and the respective expression
1252 of these ORF (Log_2FC) are indicated into parenthesis with the color corresponding to that of
1253 the ORF in the cartoon. NSC, non-significantly changed.

bioRxiv preprint doi: https://doi.org/10.1101/2020.11.06.371039; this version posted November 6, 2020. The copyright holder for this preprint (which was not certified by peer review) is the author/funder, who has granted bioRxiv a license to display the preprint in perpetuity. It is made available under aCC-BY 4.0 International license.

A



B

```
BsFur       ----------------MENRIDRIKKQLHSSSYKLTPQREATVRVLLENEEDHLSAEDVY    44
BsPerR      ----------------MAAHELKEALETLKETGVRITPQRHAILEY-LVNSMAHPTADDIY    44
10155       ----------------MKDSYERSKKILEDAGINVTVQRLQMANL-LLSKPQHLTADQVF    43
05620       -----MESLFAKKVCL---TPVEIERRLKSVSIQPTIQRISICQY-VLCEADHPTAEVVK    51
04825       MNREKQEAILNKTQPAVRMEMQTFSEYLQKEGLKITNQRMLVAER-IFSLHNHFTAEGLL    59
18590       MSLEEYLKAIYELSLNNEKVSTNSIAEKLGVSPASVTEMVQKLEK-KELIHYEKYKGVIL    59

BsFur       LLVKEKSPEIGLATVYRTLELLTELKVVDKINFGD-GVSRYDLRKEGAAHFHHHLVCMEC   103
BsPerR      KALEGKFPNMSVATVYNNLRVFRESGLVKELTYGD-ASSRFDFVT----SDHYHAICENC    99
10155       QLINEHMPNASRATIFNNLKLFAEKGIVNLLELKS-GITLYDSNV----VHHHHAIDEKT    98
05620       EWVDSRSFKMSLATVYNTLNILVSAGLLREFKFSCLGKSVYDSNI----IDHYHFFDEKS   107
04825       EEFKDQRDQISKATIYRILSIMVSAGLLQEHNFGK-DYKYYEHIIG--HKHHDHIICTVC   116
18590       ELSRKNLDNLGIATVYRAVNHLMETGTIHEIHLPG-ESSRFEASR----HHHHHFHCKQC    89

BsFur       GAVDEIEEDLLEDVEEIIERDWKFKIKDHRLTFHGICHRCNGK------ETE- 149
BsPerR      GKIVDFHYPGLDEVEQLAAHVTGFKVSHHRLEIYGVCQECSKK------ENH- 145
10155       GEIYDISLDSKLQEKVLSELKQDFKLKTGSS-----LENCNLSITLKGKKNP- 145
05620       GKFHDIDPSLLSL---SSKLPPEFLVNKTDILLTGNLVSET---------- 145
04825       GKIVEFLDERIEQLQEQAAKENGFKITGHSLNIYGTCNEHSSS------K--- 160
18590       DRVYDIEICPI----PLDKSPKGFTVDTHEIILYGTCSDCNSK------AR-- 130
```

C

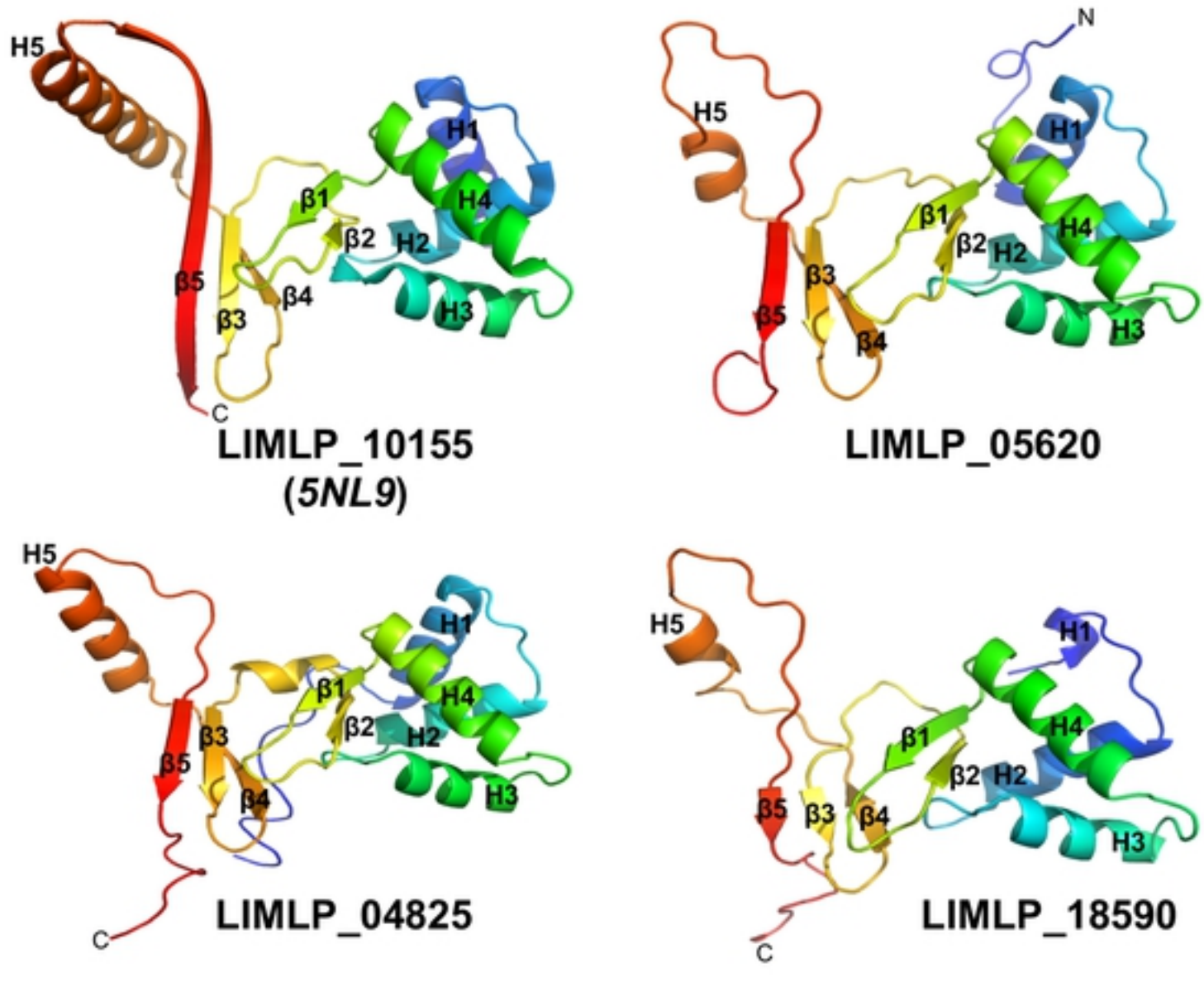


Fig 1

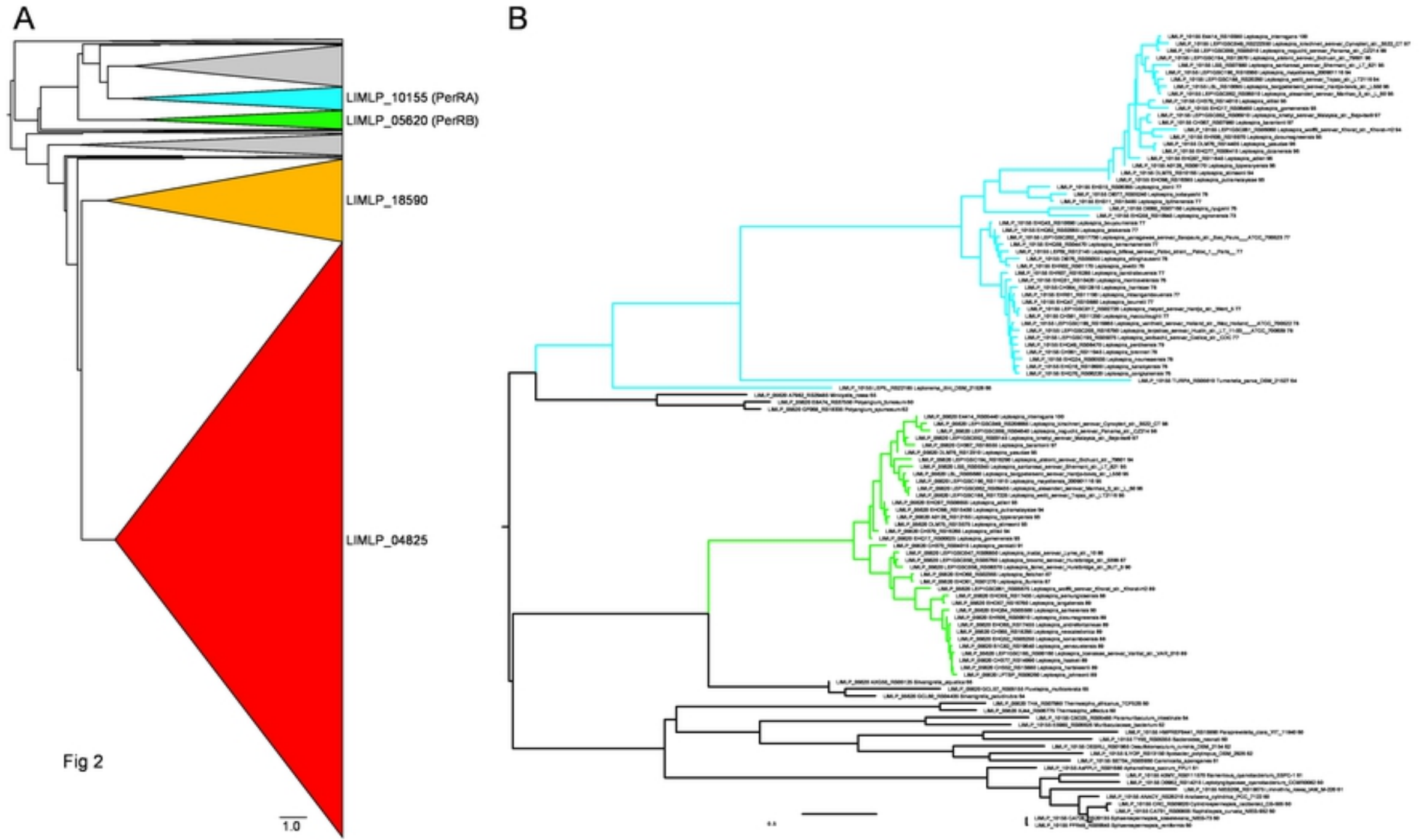
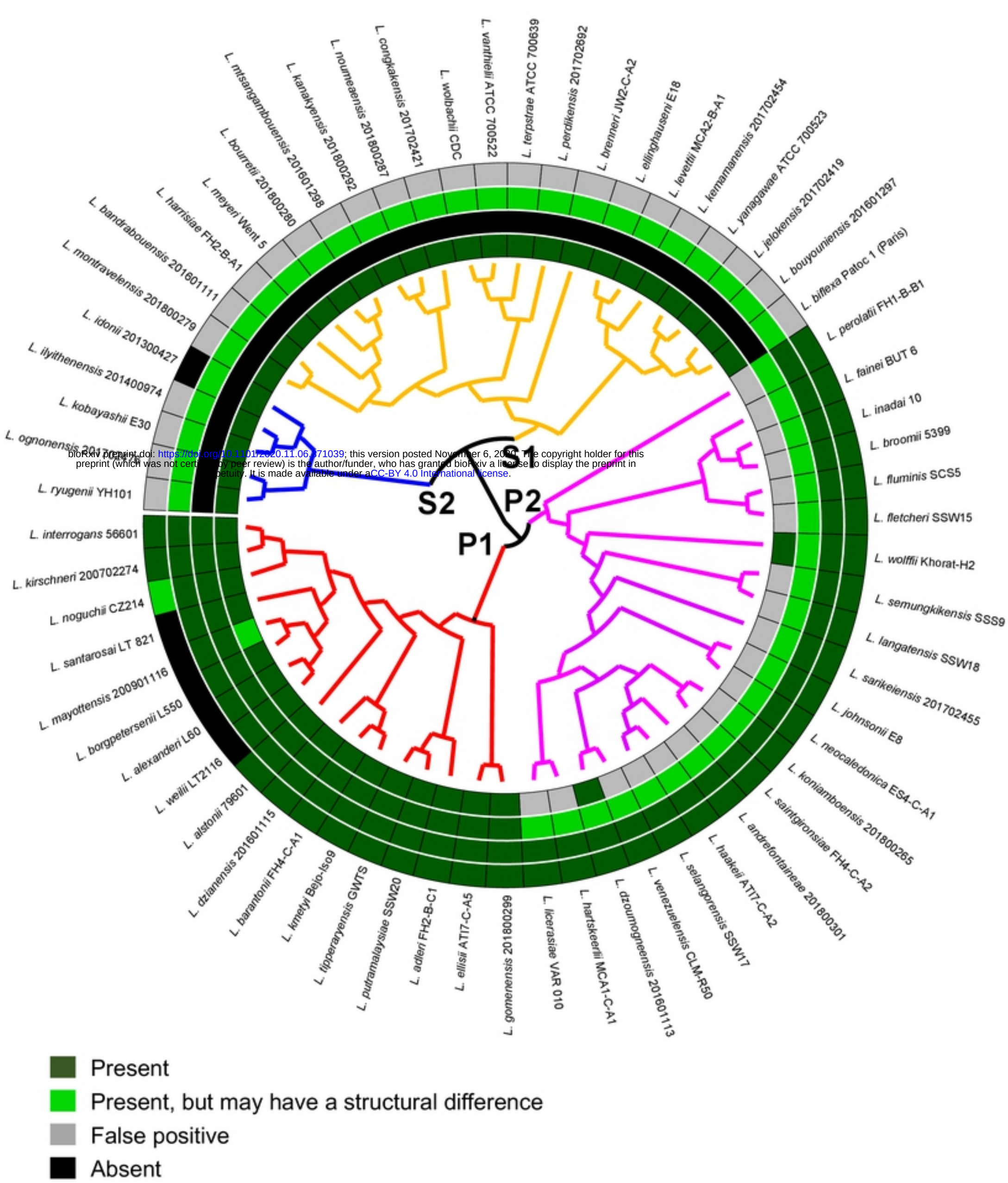

A
LIMLP_10155 (PerRA)
LIMLP_05620 (PerRB)
LIMLP_18590
LIMLP_04825
1.0
B

Fig 2

bioRxiv preprint doi: https://doi.org/10.1101/2020.11.06.371039; this version posted November 6, 2020. The copyright holder for this preprint (which was not certified by peer review) is the author/funder, who has granted bioRxiv a license to display the preprint in perpetuity. It is made available under aCC-BY 4.0 International license.



Present
Present, but may have a structural difference
False positive
Absent

Fig 3

bioRxiv preprint doi: https://doi.org/10.1101/2020.11.06.371039; this version posted November 6, 2020. The copyright holder for this preprint (which was not certified by peer review) is the author/funder, who has granted bioRxiv a license to display the preprint in perpetuity. It is made available under aCC-BY 4.0 International license.

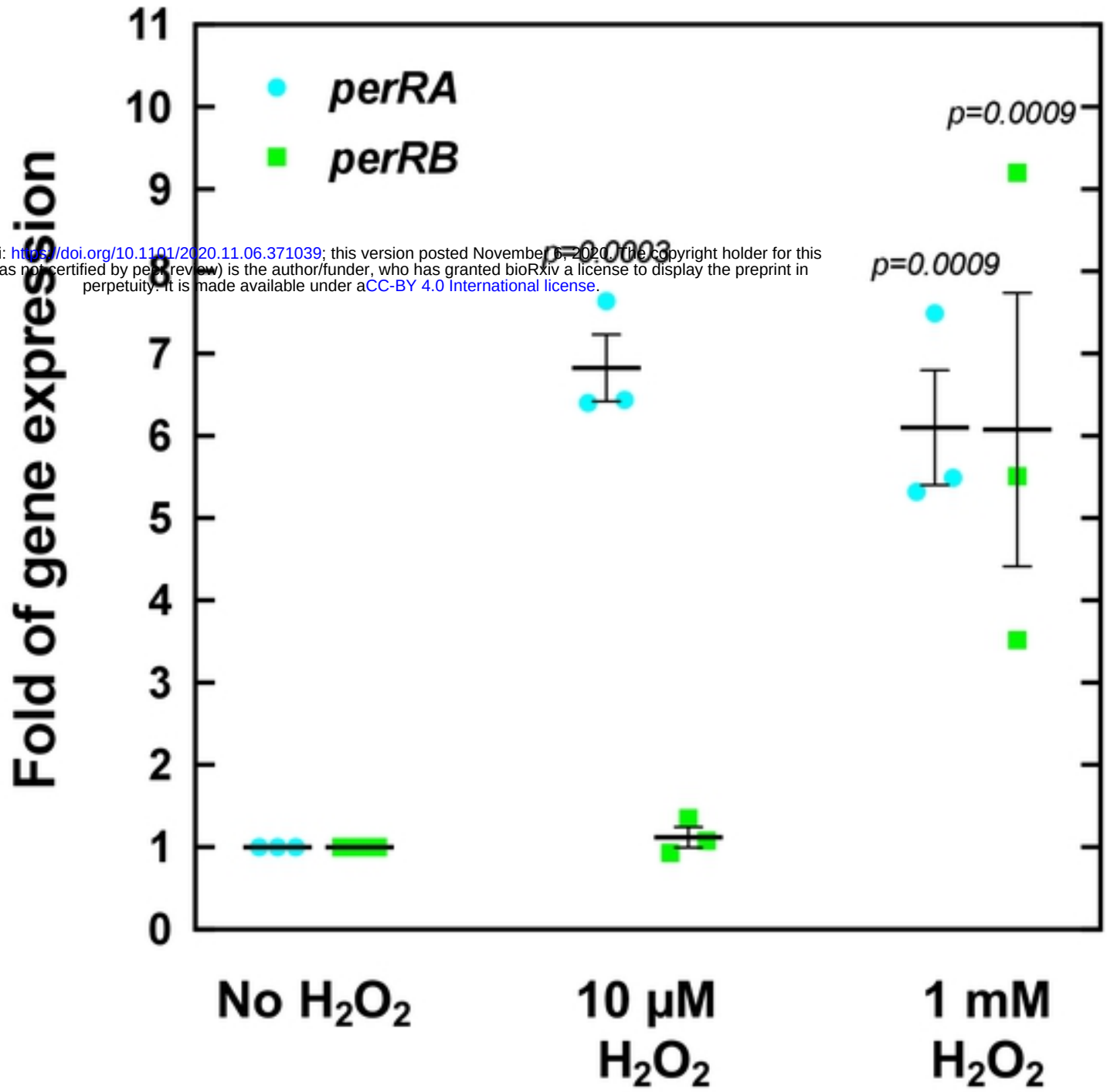


Fig 4

bioRxiv preprint doi: https://doi.org/10.1101/2020.11.06.371039; this version posted November 6, 2020. The copyright holder for this preprint (which was not certified by peer review) is the author/funder, who has granted bioRxiv a license to display the preprint in perpetuity. It is made available under aCC-BY 4.0 International license.

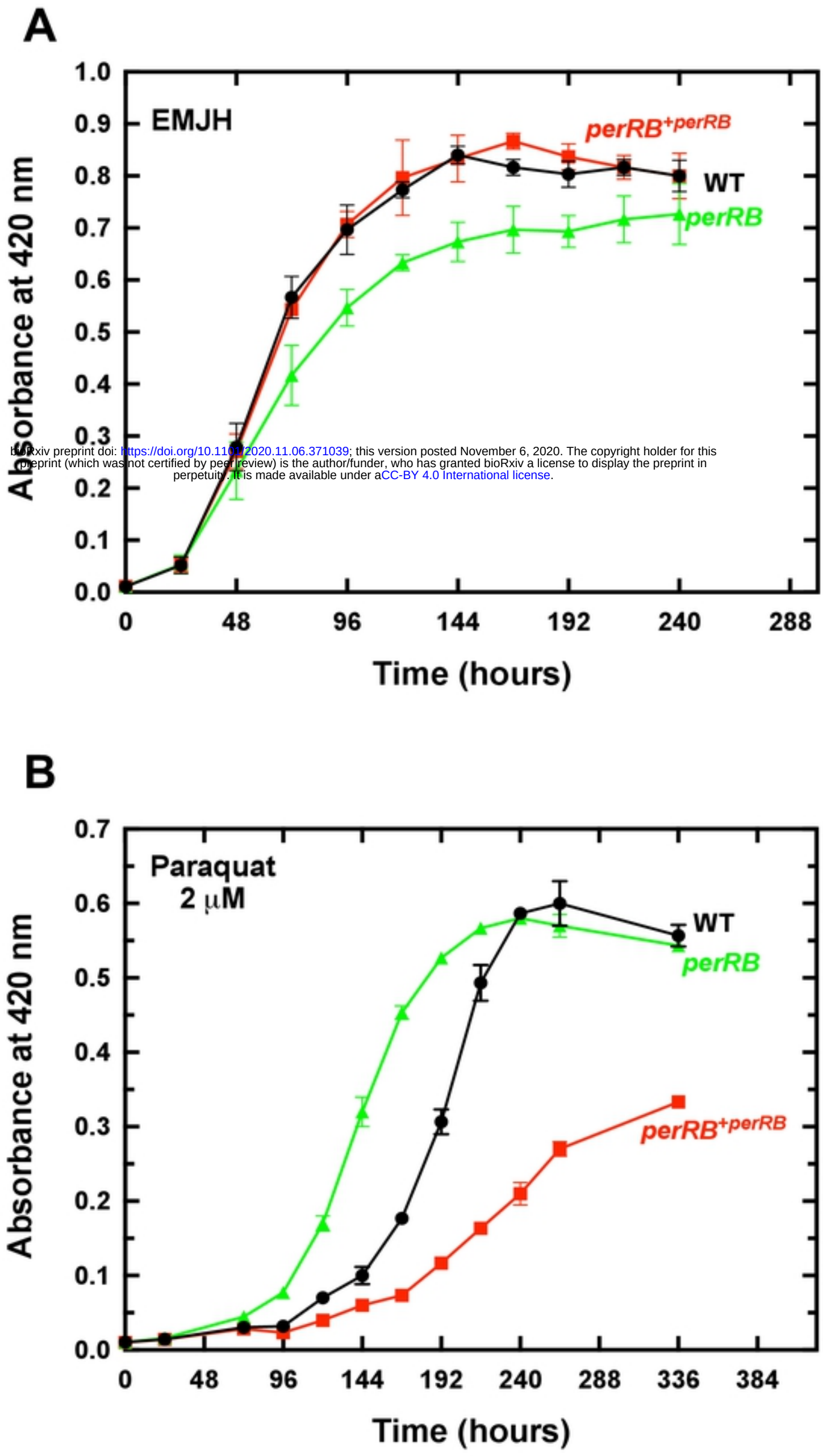
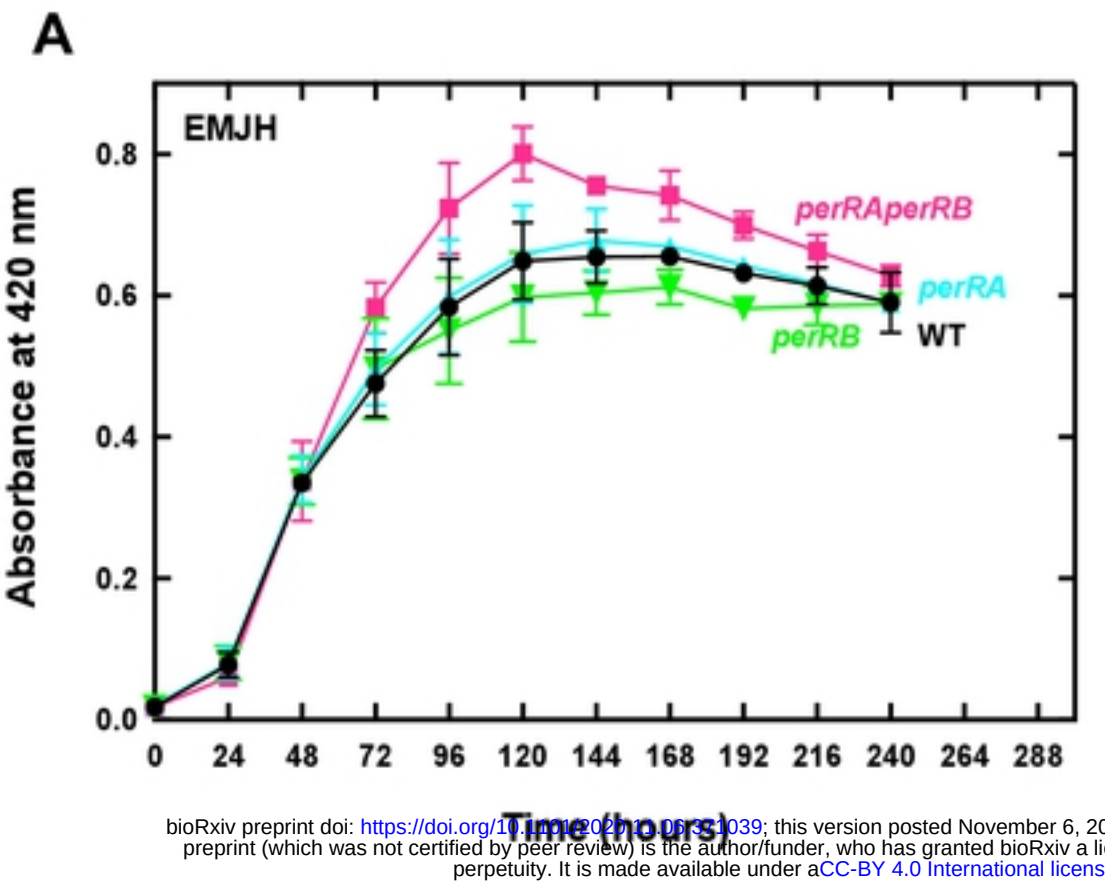
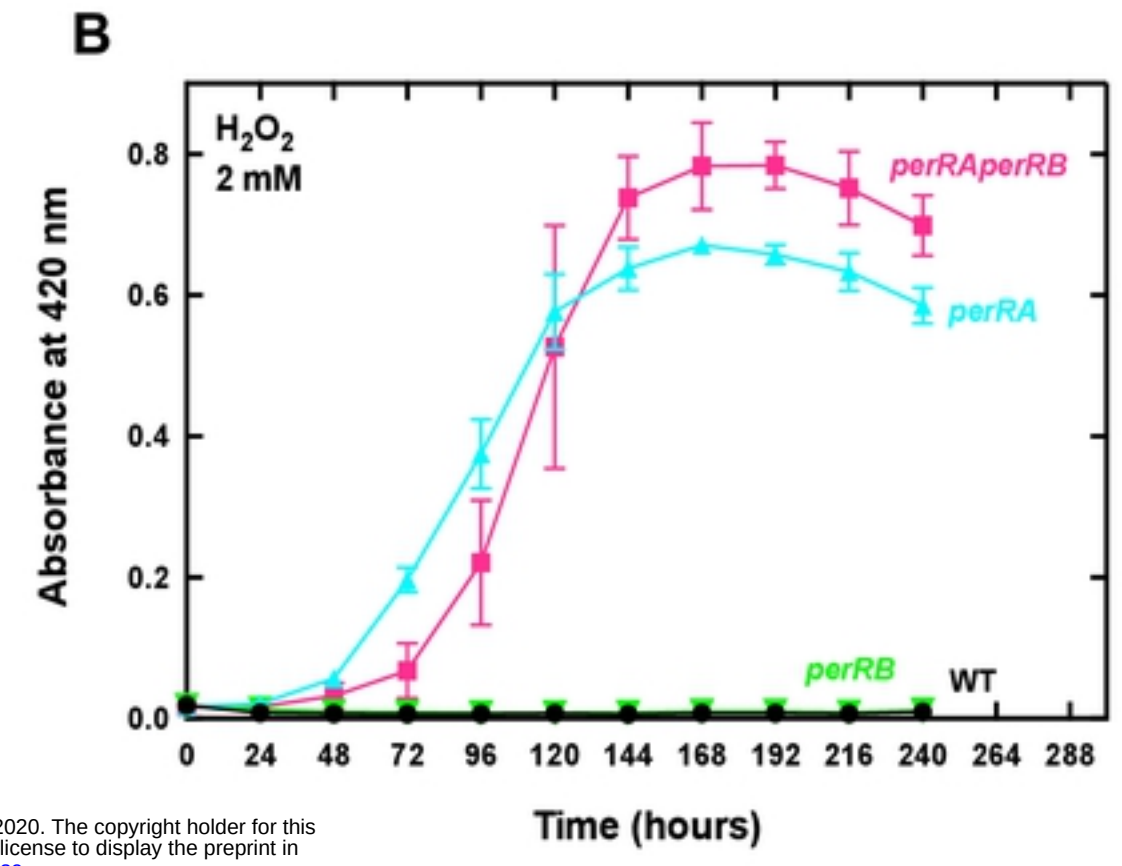
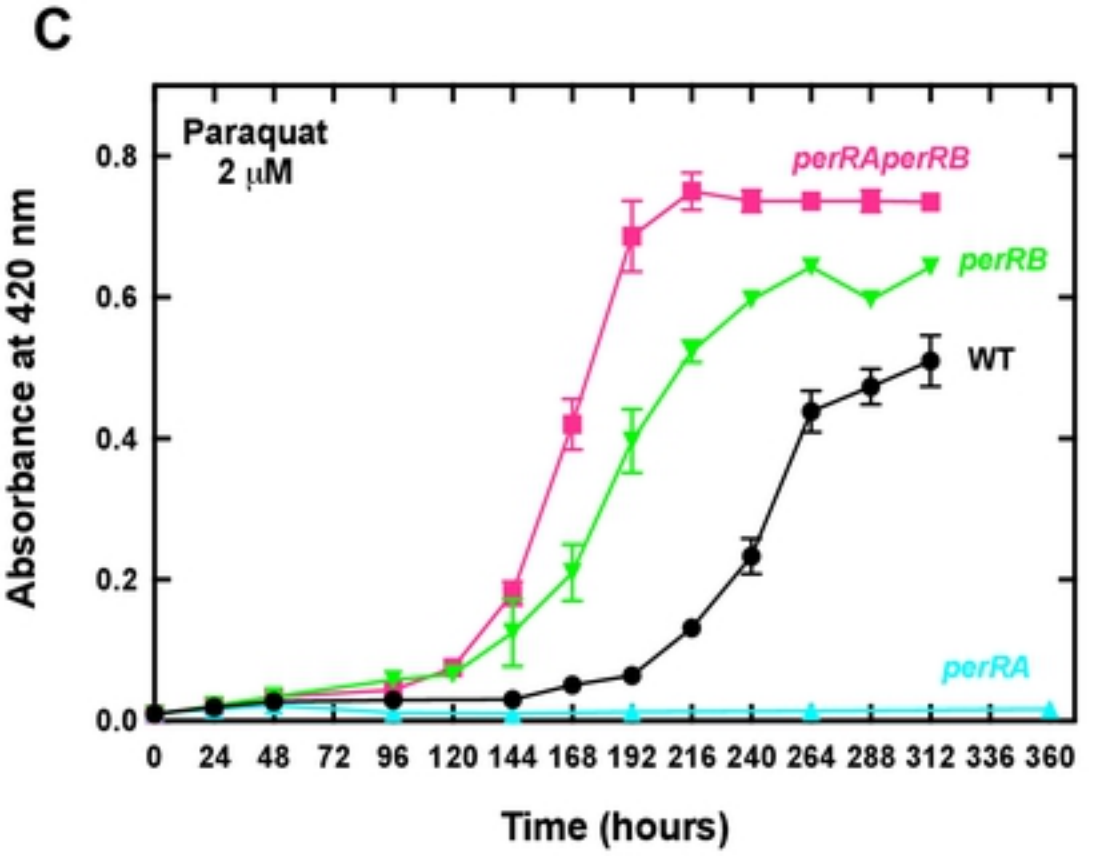


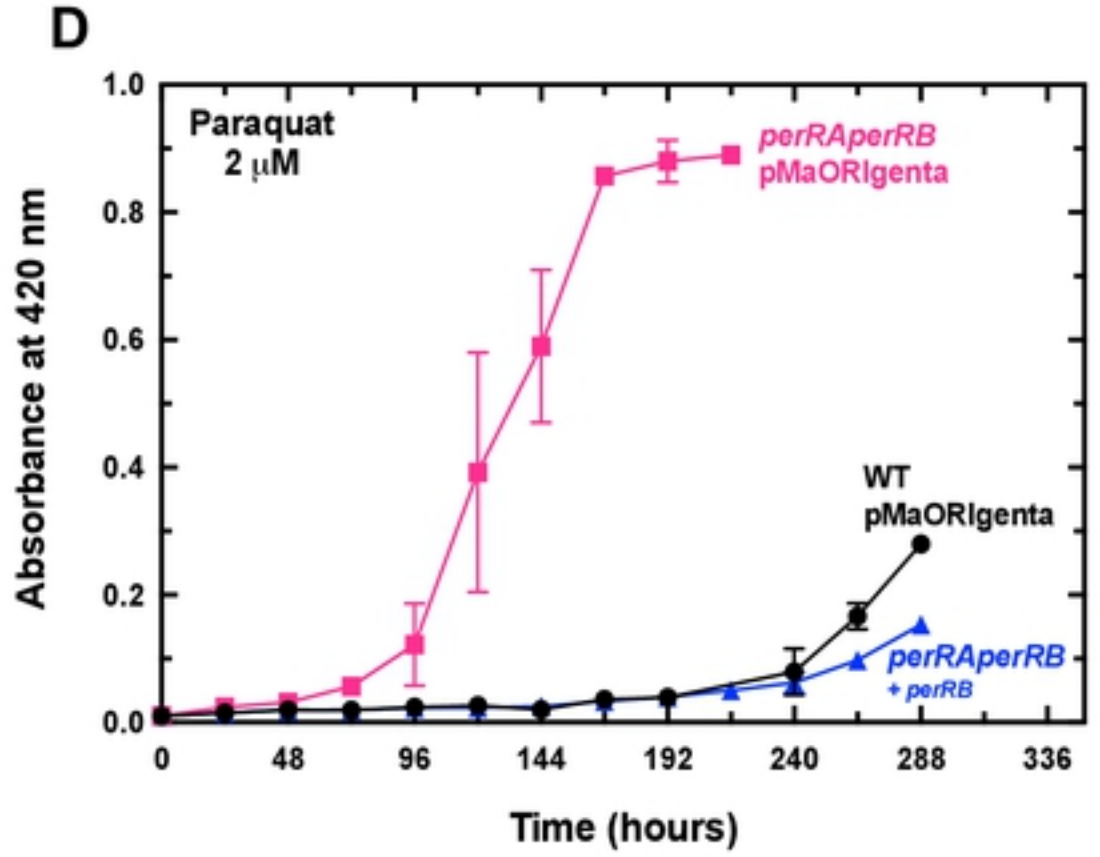
Fig 5

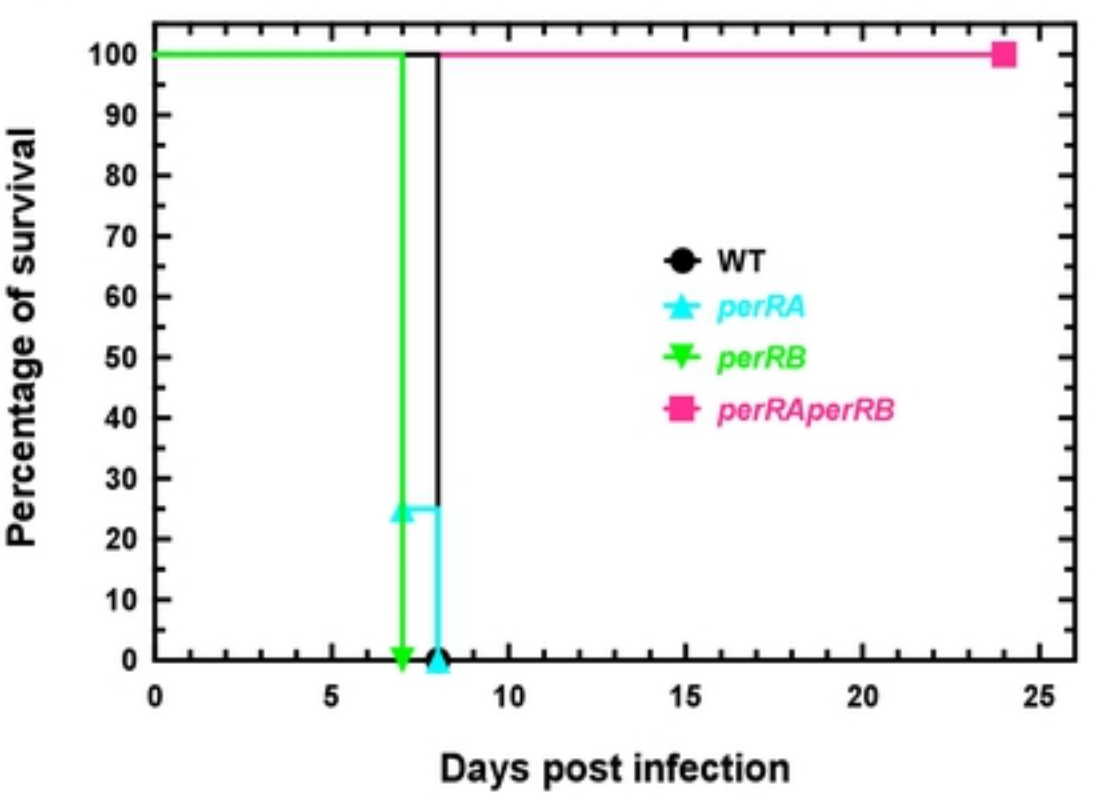
bioRxiv preprint doi: https://doi.org/10.1101/2020.11.06.371039; this version posted November 6, 2020. The copyright holder for this preprint (which was not certified by peer review) is the author/funder, who has granted bioRxiv a license to display the preprint in perpetuity. It is made available under aCC-BY 4.0 International license.











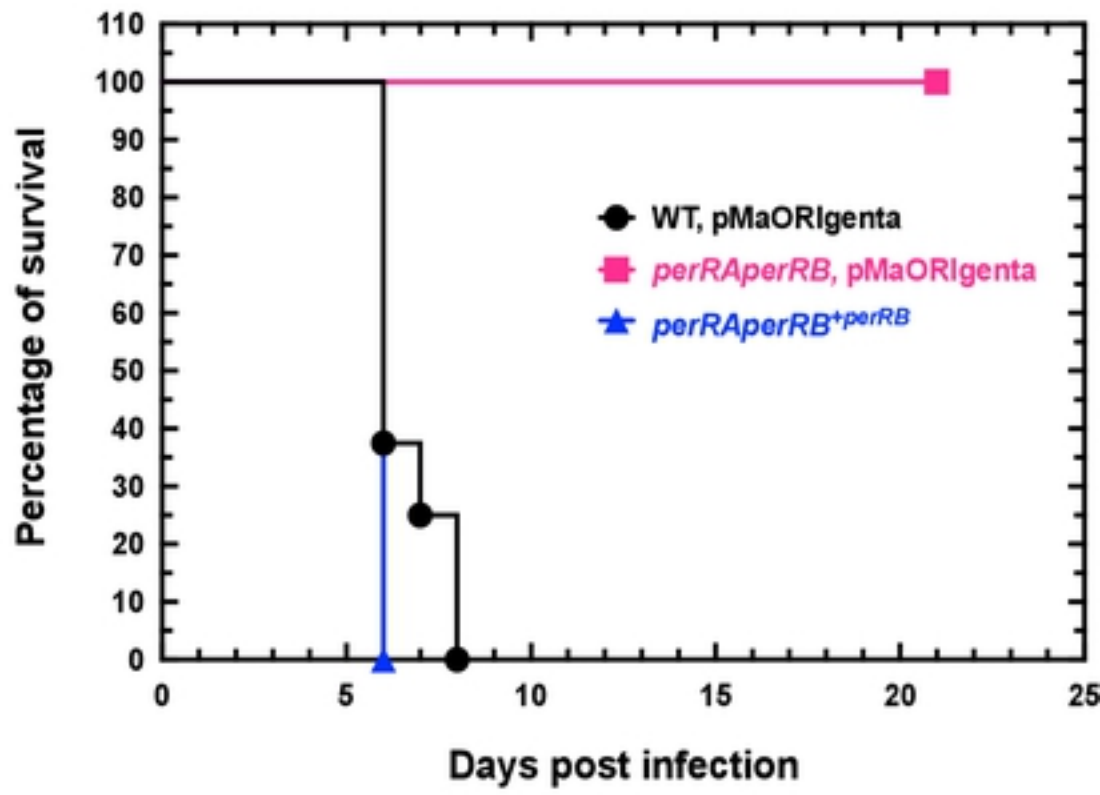


Fig 6

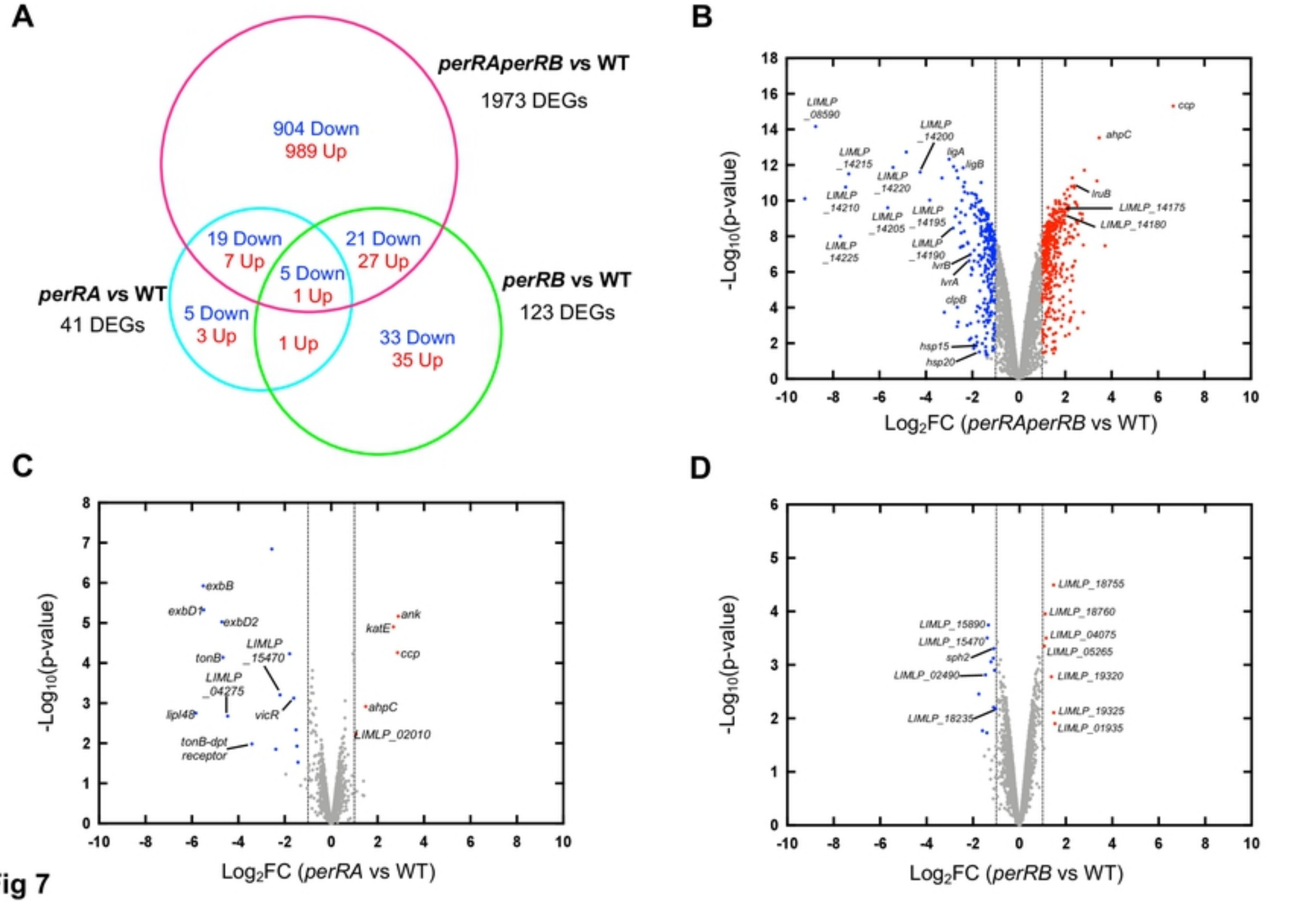

A
perRAperRB vs WT
1973 DEGs
904 Down
989 Up
19 Down
7 Up
21 Down
27 Up
5 Down
1 Up
perRA vs WT
41 DEGs
5 Down
3 Up
1 Up
perRB vs WT
123 DEGs
33 Down
35 Up
B
-Log10(p-value)
Log2FC (perRAperRB vs WT)
LIMLP_08590
LIMLP_14200
LIMLP_14215
LIMLP_14220
LIMLP_14210
LIMLP_14205
LIMLP_14195
LIMLP_14190
LIMLP_14225
ligA
ligB
lvrB
lvrA
clpB
hsp15
hsp20
ccp
ahpC
lruB
LIMLP_14175
LIMLP_14180
C
-Log10(p-value)
Log2FC (perRA vs WT)
exbB
exbD1
exbD2
tonB
LIMLP_15470
LIMLP_04275
lipl48
vicR
tonB-dpt receptor
ank
katE
ccp
ahpC
LIMLP_02010
D
-Log10(p-value)
Log2FC (perRB vs WT)
LIMLP_15890
LIMLP_15470
sph2
LIMLP_02490
LIMLP_18235
LIMLP_18755
LIMLP_18760
LIMLP_04075
LIMLP_05265
LIMLP_19320
LIMLP_19325
LIMLP_01935

Fig 7

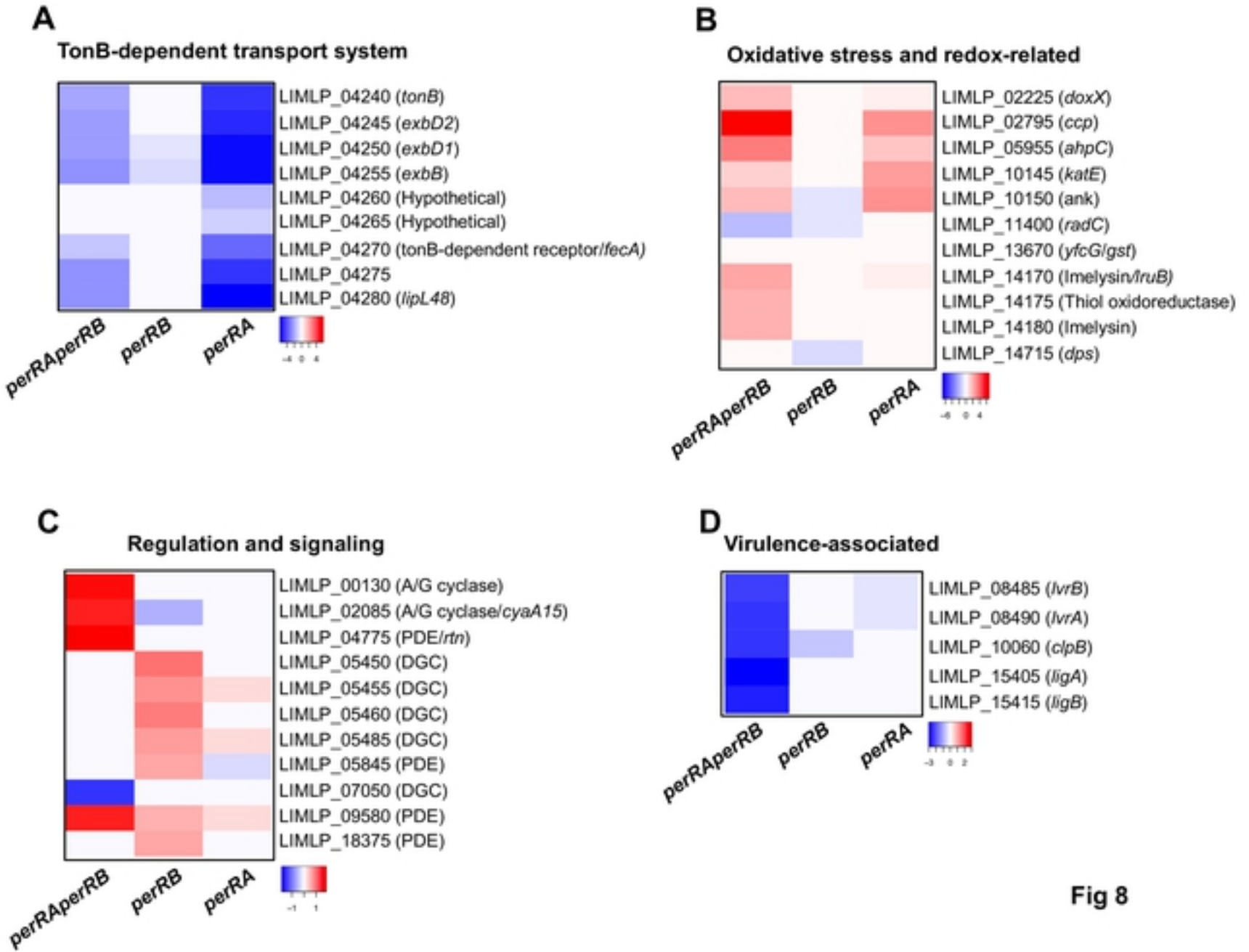

A
TonB-dependent transport system
LIMLP_04240 (tonB)
LIMLP_04245 (exbD2)
LIMLP_04250 (exbD1)
LIMLP_04255 (exbB)
LIMLP_04260 (Hypothetical)
LIMLP_04265 (Hypothetical)
LIMLP_04270 (tonB-dependent receptor/fecA)
LIMLP_04275
LIMLP_04280 (lipL48)
perRAperRB
perRB
perRA
B
Oxidative stress and redox-related
LIMLP_02225 (doxX)
LIMLP_02795 (ccp)
LIMLP_05955 (ahpC)
LIMLP_10145 (katE)
LIMLP_10150 (ank)
LIMLP_11400 (radC)
LIMLP_13670 (yfcG/gst)
LIMLP_14170 (Imelysin/truB)
LIMLP_14175 (Thiol oxidoreductase)
LIMLP_14180 (Imelysin)
LIMLP_14715 (dps)
perRAperRB
perRB
perRA
C
Regulation and signaling
LIMLP_00130 (A/G cyclase)
LIMLP_02085 (A/G cyclase/cyaA15)
LIMLP_04775 (PDE/rtn)
LIMLP_05450 (DGC)
LIMLP_05455 (DGC)
LIMLP_05460 (DGC)
LIMLP_05485 (DGC)
LIMLP_05845 (PDE)
LIMLP_07050 (DGC)
LIMLP_09580 (PDE)
LIMLP_18375 (PDE)
perRAperRB
perRB
perRA
D
Virulence-associated
LIMLP_08485 (lvrB)
LIMLP_08490 (lvrA)
LIMLP_10060 (clpB)
LIMLP_15405 (ligA)
LIMLP_15415 (ligB)
perRAperRB
perRB
perRA

Fig 8

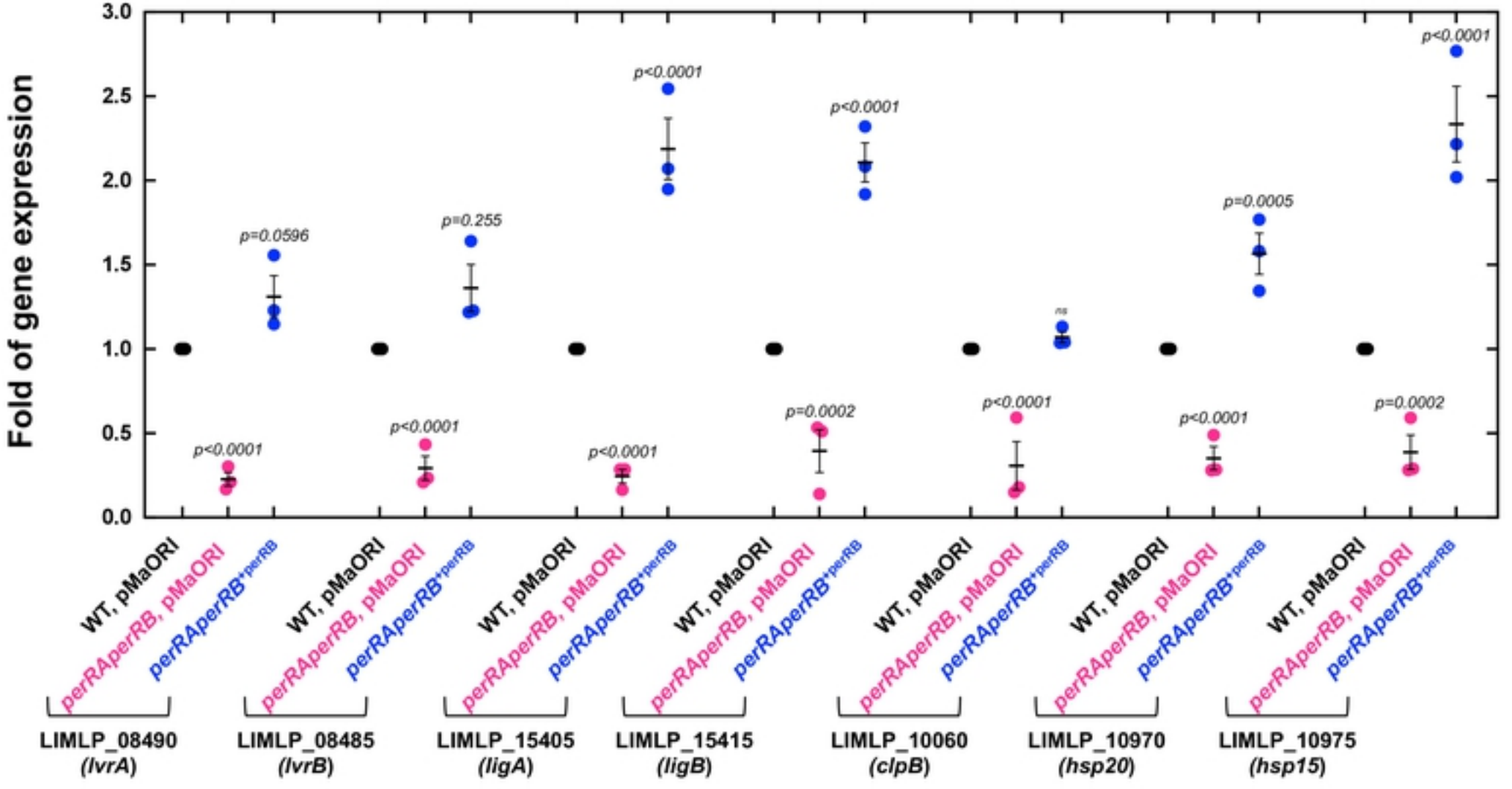

Fold of gene expression
3.0
2.5
2.0
1.5
1.0
0.5
0.0
p<0.0001
p=0.0596
p<0.0001
p<0.0001
p=0.255
p<0.0001
p<0.0001
p<0.0001
p=0.0002
p<0.0001
ns
p<0.0001
p=0.0005
p<0.0001
p<0.0001
p=0.0002
p<0.0001
WT, pMaORI
perRAperRB, pMaORI
perRAperRB+perRB
LIMLP_08490 (lvrA)
LIMLP_08485 (lvrB)
LIMLP_15405 (ligA)
LIMLP_15415 (ligB)
LIMLP_10060 (clpB)
LIMLP_10970 (hsp20)
LIMLP_10975 (hsp15)

Fig 9

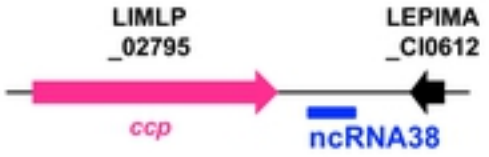
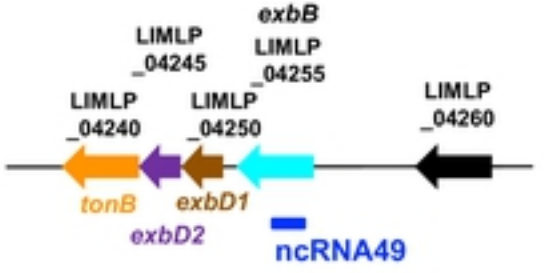
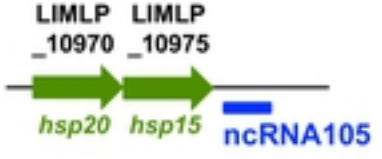
	perRAperRB vs WT[a]	*perRA* vs WT[b]	*perRB* vs WT[a]	H2O2[b]
	5.96 (6.71)	2.50 (2.77)	NSC	4.25 (5.82)
	-1.51 (-2, -2.3, -2.3, -2.5)	NS	NSC	NS
	-1.18 (-2.27)	NS	NSC	7.19 (6.79, 6.59)
	-2.62 (-2.25, -0.62)	NS	NSC	2.13 (1.76, -0.25)

Fig 10